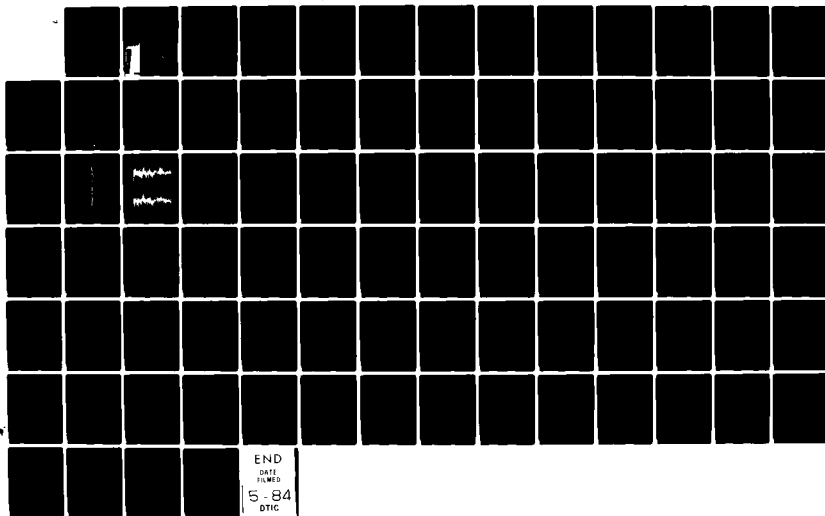
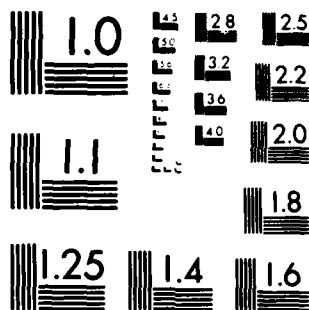


AD-A138 694

NEW TECHNIQUES FOR MEASURING SINGLE EVENT RELATED BRAIN  
POTENTIALS..(U) PURDUE UNIV LAFAYETTE IN SCHOOL OF  
ELECTRICAL ENGINEERING C D MCGILLEM ET AL. 15 OCT 83 1/1  
AFOSR-TR-84-0127 AFOSR-80-0152 F/G 12/1 NL

UNCLASSIFIED





AFOSR-TR-84-0127

3

AD A138694

## New Techniques for Measuring Single Event Related Brain Potentials

C. D. McGillem  
J. I. Aunon

October 1983

DTIC FILE COPY

DTIC  
S  
MAR 7 1984  
A

School of Electrical Engineering  
Purdue University  
West Lafayette, Indiana 47907

84 03 06 146

Approved for public release;  
distribution unlimited.

UNCLASSIFIED

SECURITY CLASSIFICATION OF THIS PAGE (When Data Entered)

REPORT DOCUMENTATION PAGE		READ INSTRUCTIONS BEFORE COMPLETING FORM
1. REPORT NUMBER <b>AFOSR-TR- 84-0127</b>	2. GOVT ACCESSION NO. <b>AD-A138694</b>	3. RECIPIENT'S CATALOG NUMBER
4. TITLE (and Subtitle) New Techniques for Measuring Single Event Related Brain Potentials		5. TYPE OF REPORT & PERIOD COVERED <b>FINAL REPORT</b>
		6. PERFORMING ORG. REPORT NUMBER
7. AUTHOR(s) C. D. McGillem J. I. Aunon		8. CONTRACT OR GRANT NUMBER(s)  AFOSR-80-0152
9. PERFORMING ORGANIZATION NAME AND ADDRESS School of Electrical Engineering Purdue University W. Lafayette, IN 47907		10. PROGRAM ELEMENT, PROJECT, TASK AREA & WORK UNIT NUMBERS  61102F 2313/A4
11. CONTROLLING OFFICE NAME AND ADDRESS Air Force Office of Scientific Research/NL Bolling AFB, DC 20332		12. REPORT DATE 10/15/83
		13. NUMBER OF PAGES 83
14. MONITORING AGENCY NAME & ADDRESS (if different from Controlling Office)		15. SECURITY CLASS. (of this report)  Unclassified
		15a. DECLASSIFICATION/DOWNGRADING SCHEDULE
16. DISTRIBUTION STATEMENT (of this Report)  Approved for public release; distribution unlimited.		
17. DISTRIBUTION STATEMENT (of the abstract entered in Block 20, if different from Report)		
18. SUPPLEMENTARY NOTES		
19. KEY WORDS (Continue on reverse side if necessary and identify by block number)  Event related potential; evoked potential, pattern classification; linear discriminant analysis, quadratic discriminant analysis, data preprocessing, visual evoked potential.		
20. ABSTRACT (Continue on reverse side if necessary and identify by block number)  → Methods for selecting features of evoked potential (EP) waveforms to improve classification accuracy are described. It is found that use of an exhaustive search procedure gives moderate improvement over forward sequential feature selection and stepwise linear discriminant analysis procedures. A new procedure for classification using a combination of temporal and spectral representations of the data is described.  Experimental results are presented illustrating the effectiveness of		

DD FORM 1 JAN 73 1473 EDITION OF 1 NOV 65 IS OBSOLETE

UNCLASSIFIED  
SECURITY CLASSIFICATION OF THIS PAGE (When Data Entered)

*Unclassified*

SECURITY CLASSIFICATION OF THIS PAGE (When Data Entered)

Block 20 (continued)

time-varying filters for processing EP waveforms. It is shown by means of computer simulations that much greater noise reduction is obtained with time-varying filters than is possible by any of the more conventional procedures that utilize time-invariant filters. At the same time the underlying waveforms are preserved by the filtering process.

Modifications of a computer controlled display system to give precise timing measurements are described. Data showing the reduction in latency variance of EP components are presented. Reductions in the standard deviations of about 20% were obtained.

Experimental measurements of EP waveforms using a Sternberg paradigm are described. Preliminary analysis of the results shows an apparent substructure in the P300 and a significant correlation of certain of the P300 components and reaction time.

Accession For	
TAR	
Classification	
P.	
Distribution/	
Availability Notes	
Dist	Special
A1	

100-1000000

UNCLASSIFIED

## RESEARCH OBJECTIVES

The research reported herein is concerned with improved information extraction from single evoked brain potential waveforms. Currently research is being carried out in the following areas.

- a. Study of methods for increasing accuracy of classifying evoked potential (EP) waveforms through optimized feature selection and appropriate preprocessing of the data.
- b. Investigation of single EP processing and filtering techniques to provide improved waveform estimation.
- c. Investigation of the detailed structure of EP waveform components related to cognitive processing of sensing input data.

## SUMMARY OF RESEARCH RESULTS

### Improved Classification of Evoked Potential Waveforms

*Exhaustive Search Feature Selection.* As discussed in the last report, a series of tests were run to determine how much improvement is possible in automated classification when an optimum feature set is employed. These results were extended by carrying out an evaluation procedure using the "leaving-one-out" method which provides a lower bound on performance of the classifier. The paradigm employed was described in the previous report and consisted of presentation of a sequence of letter V's with random interstimulus intervals and the random insertion (0.1 probability) of an inverted letter (IV). The EP waveform was recorded at electrodes Oz, Pz and Cz. Time samples 20 ms apart were used as the feature set and upper and lower bounds on accuracy of classification were determined. The upper bound (UB) was taken to be the performance when training and testing were done on the same data set and the lower bound (LB) was taken to be the performance when the leaving-one-out method was used. Table 1 gives the performance of four classifiers employing five time samples

Table 1: Classification accuracies (%)

Electrode	Subject	FSFS (linear)		FSFS (quadratic)		SLDA		ESFS	
		UB	LB	UB	LB	UB	LB	UB	LB
Oz	1	86%	85%	88%	86%	86%	84%	88%	85%
	2	89%	85%	90%	89%	84%	83%	88%	85%
	4	85%	83%	89%	84%	80%	79%	84%	83%
	5	83%	79%	89%	85%	81%	76%	85%	79%
Pz	1	85%	84%	91%	89%	93%	88%	93%	88%
	2	88%	85%	90%	84%	86%	83%	91%	88%
	4	83%	75%	91%	89%	83%	80%	89%	85%
	5	78%	78%	83%	78%	76%	73%	81%	76%
Cz	1	78%	70%	89%	80%	75%	73%	81%	78%
	2	86%	85%	89%	86%	84%	83%	86%	85%
	4	83%	83%	88%	83%	80%	80%	83%	83%
	5	75%	73%	86%	83%	73%	70%	75%	73%

selected in accordance with methods appropriate to that procedure. The classification procedures used were: linear discriminant function with forward sequential feature selection (FSFS (linear)); quadratic discriminant function with forward sequential feature selection (FSFS (quadratic)); step-wise linear discriminant analysis (SLDA); linear discriminant function with exhaustive search feature selection (ESFS).

Exhaustive feature selection algorithms typically require many hours of computer time to select five features. The best implementation of ESFS employed in this study required 34 minutes. This is on the order of 100 to 1000 times faster than typical implementations. The final version is about 10 times slower than the suboptimal feature selection algorithms which normally require 2 to 5 minutes of computer time. It must be emphasized that to realize the speed of this or any exhaustive algorithm, the number of features in the data records should be as small as possible.

The classification accuracies listed in Table 1 show that in general the ESFS algorithm results in a 2-3% improvement in classification accuracy over the linear suboptimal algorithms. The classification accuracies in all cases were high suggesting that ERPs from a VIV paradigm are indeed easily linearly separable. Note that since both the upper and lower bounds were considered in determining the best feature set, there are three examples where a suboptimal algorithm (FSFS linear) did better on one of the error bounds. In subjects 2 and 4 for electrode Oz the upper bound was better and in subject 5 for electrode Pz the lower bound was better. The case where both bounds were better for the linear suboptimal algorithms never occurred. The best improvements were 3-8% using data from electrode Pz. This is expected since the P300 is a maximum in the parietal region of the brain. The best accuracy bounds were also found for data from electrode Pz. The ESFS classification accuracy (excluding subject 5) was bounded between 85% and 93%. These results are comparable to the quadratic FSFS and in one case are better.

**AIR FORCE OFFICE OF SCIENTIFIC RESEARCH (AFOSR)**  
**NOTICE OF TRANSMITTAL TO DTIC**  
 This technical report has been prepared by the  
 AFOSR and is being submitted to DTIC for distribution.  
 Distribution is unlimited.  
**MATTHEW J. K. [illegible]**  
**Chief, Technical Information Division**



The quadratic FSFS algorithm performed very well. There were significant improvements in the lower bounds even over ESFS in most cases. This fact raised the question of how well a quadratic ESFS algorithm would perform. Because the exhaustive quadratic algorithm cannot be implemented efficiently, however, it was not investigated. The performance of the quadratic FSFS algorithm suggests that it would be preferable to any linear exhaustive algorithm for both classification accuracy and speed.

*Preprocessing for Improved Classification Accuracy.* Research is being carried out to investigate the use of temporal and spectral characteristics of evoked potentials to improve classification and detection accuracy and identify the underlying components and their parameters. Estimation of the frequency components over short time intervals helps identify time varying components in the signal. If a particular frequency component or band of frequencies is found to be prevalent or reliably detected in the same short time segments of signals from an ensemble of data, that portion may be represented by a component in a space of finite duration sinusoidal basis functions. Since the data segment is finite, the mapping will be onto a portion of a sinusoid whose phase must also be determined.

The basic EEG components are modeled as a sum of windowed sinusoids. If several segments of the signal are found which reliably map to various sinusoidal frequencies with a similar phase from the analysis of an ensemble of EP data, then that portion of the signal may be considered to be a summation of the various sinusoidal segments located at different latencies:

$$s(t) = \sum_{i=1}^N \sin(2\pi f_i t + \phi_i) w(t - t_i)$$

where the signal  $s(t)$  is a summation of individual components which are segments of the sine waves at frequencies  $f_i$  with phase  $\phi_i$ , windowed about time  $t_i$  with an appropriate windowing function. This windowing function will depend on the actual spectrum about the frequency  $f_i$ . It will alter the sinusoid by diminishing its amplitude

at the ends of the segment from which it is mapped. Outside the segment it would be considered to be zero or diminish to zero within a short interval. Many forms of components may be considered by using different sinusoidal components and windowing functions which may be estimated from the average spectrum of the data.

The present research tests the efficacy of using selected amplitudes from the time-frequency plane, or equivalently, portions of the real part of the time-varying spectrum, as features in classifiers to distinguish brain evoked potentials. Previous work has focused on features taken from one dimensional systems, mainly amplitudes from the time dimension or axis and magnitude and phases from the frequency dimension. When features were selected from the time and frequency dimensions, the geometrical relationship between these dimensions was not considered to form a two-dimensional space. The amplitudes along the time and frequency dimensions were not taken in pairs but singly, hence the features were selected from a larger number of possible one-dimensional features.

The advantage that the one-dimensional features have over 2-dimensional features is the lesser computational time complexity involved with 1-dimensional features. For the example of  $n$  time features and  $m$  frequency features from which to select, the time complexity of 1-dimensional features is  $O(n+m)$  and 2-dimensional features is  $O(n \cdot m)$ , where  $O(\cdot)$  describes the order of the magnitude of the complexity and is proportional to the term in parenthesis, which is the highest order parametric term of the computation time equation. This results in a very large differential in the computational time if the number of features is large for high resolution within the dimensions. The large computational burden of many types of feature selection processes has restricted research of the 2-dimensional time-frequency plane.

Amplitudes at particular times, or at particular latencies of the evoked potential, contain energy from a wide range of frequencies unless the signal has been significantly filtered. In past work, the filtering usually involved low pass filtering, which allows a

wide band of frequencies to be passed. This band may typically be 0.1 Hz to 25 Hz. Frequency features, either magnitude or phase, represent energy at a particular frequency from the expected duration of the signal or evoked potential. If the amplitude at a particular time was measured from the signal after being filtered to allow only a narrow band of frequencies to pass, this would approximate the amplitude of a region of the time-frequency plane. This corresponds with frequency features which represent energy at a particular frequency from a particular segment of the signal or the real part of a frequency component at a particular time from the time-varying spectrum. Various segments of the signal correspond to regions along the time axis of the time-frequency plane. The frequencies of the signal that the narrowband filters pass correspond to regions along the frequency axis.

Continuing research will investigate the features representing amplitudes on the time-frequency plane for classification and detection of single evoked potentials. A 2-step feature selection/classification procedure as outlined in Figure 1 is being developed and tested. This process first transforms the windowed signals into frequency components, magnitude and phase, then selects the best frequency features using the training set signals. The set of frequencies that is selected contains signal energy or information useful to the classifier to produce low error rates. Most frequency features not selected contain energy or information not useful in the classification process, and therefore add to the variance. The selected frequencies are used to set parameters of a set of filters which will process the raw data. These filters, which may be considered feature transformation functions, will be designed to pass those frequencies which contain the majority of the useful information for classification, while rejecting those frequencies which contain mainly noise. Noise in this case refers to that part of the measured signal which contains no information useful for classification. It may be a combination of ongoing EEG, instrumentation noise, and signal energy which is similar between the various classes to be separated.

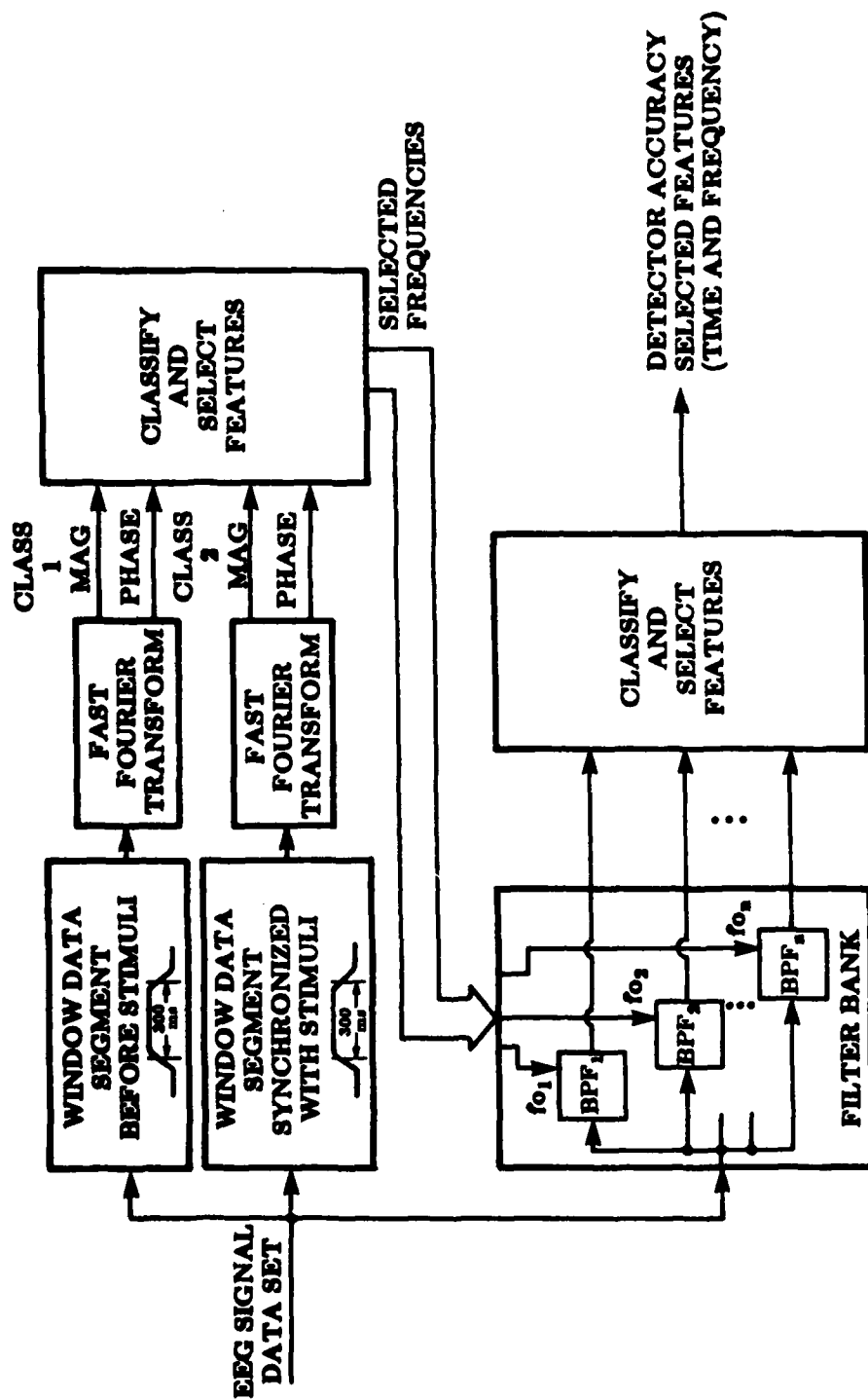


Figure 1. Block diagram of the 2-step classification/feature selection system.

The amplitudes of the outputs of these filters at various times are used as a set of features from which the classifier and feature selector routine will select a subset. The first step is classification and feature selection using the frequency components of the entire signal, selecting particular frequency lines on the time-frequency plane. The second step is filtering the signal and selecting from the set of filtered amplitude values at the sampled times (latencies). This eliminates searching the entire time-frequency plane. By restricting the search to only certain frequencies, the second step selects times at the selected frequencies, possibly eliminating some of the selected frequencies in the process. The results will be selected frequencies and times where the set of the amplitude values produce high classification accuracies.

The on-line type classifier structure which uses features previously selected is similar to the second stage of the process. It consists of a bank of filters at the frequencies selected by step -1 and maintained by step - 2. The output of these filters are used by the classifier which use selected latency adjusted amplitude features from these filtered signals to produce the desired classification. This is portrayed in Figure 2 where the example of 3 selected frequencies is shown.

#### Improved EP Waveform Estimation

Work has been completed on development of the theory of time-varying filters for improved waveform estimation. This work is described in detail in a paper to be published in the November 1983 IEEE Transactions on Biomedical Engineering.

The time varying filter is designed to process a finite duration data segment and can be thought of as an operator that maps the vector of measured values into a signal vector. The processor takes the following form

$$\hat{s}(k) = \sum_{i=1}^N h_k(i) \times x(i) = \underline{h}_k^T \underline{x} \quad k = 1, 2, \dots, N$$

where  $\hat{s}(k)$  is the estimate of the kth sample point of the signal,  $h_k(i)$  is the ith sample

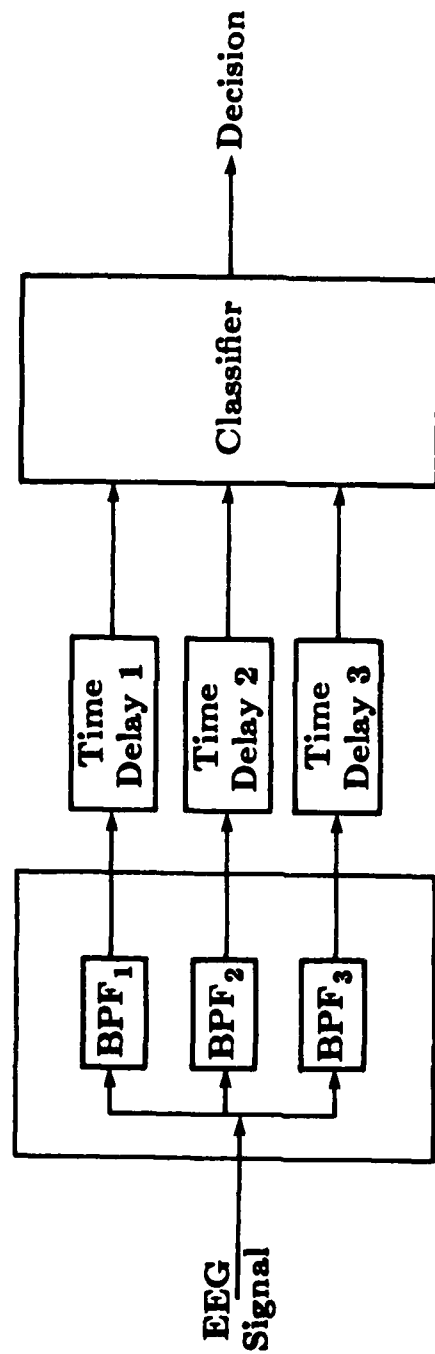


Figure 2. Block diagram of the on-line classifier or detector system. Example of a 3 filter system.

of the filter function for estimating the  $k$ th signal value and  $x(i)$  is the  $i$ th sample of the data set. Collecting the  $N$  estimators together leads to a matrix representation of the form

$$\hat{\mathbf{s}} = \mathbf{H} \mathbf{x}$$

the optimum  $\mathbf{H}$  is found as the solution to the matrix equation

$$\mathbf{H} = \mathbf{K}_{sx} \mathbf{K}_{xx}^{-1}$$

where  $\mathbf{K}_{sx}$  is the crosscovariance matrix of the signal and the data and  $\mathbf{K}_{xx}$  is the autocovariance matrix of the data.

Performance of this filter has been evaluated using simulations in which signals similar to typical average EP waveforms were combined with noise having the same spectral characteristics and amplitudes as the ongoing EEG.

The signal selected for the initial simulation study was a non-random signal corresponding to the conventional average of the observations of the evoked potential in electrode Pz elicited by 200 visual stimulations with a checkerboard pattern in the upper half visual field. The noise process is typically measured samples of the on-going EEG at the same electrode when no stimulation is present. The mean of the on-going EEG is first removed and then the noise process is scaled to obtain the desired signal-to-noise ratio. Two hundred simulations were carried out and two sets of results typical of those obtained are shown here.

Fig. 3 is the first set. In Fig. 3(a) is shown the sample observation which is the sum of the signal and noise. Fig. 3(b) is the signal estimate obtained by using the time-invariant filter. Fig. 3(c) is the signal estimate obtained by using the time-varying filter. The original signal, is also included in each plot for comparison. Fig. 4 is another set of the simulation results. In both cases a signal-to-noise ratio of -10 dB is used which is typical of SNR's occurring in evoked potential research. The time-varying filter is seen to perform much better than the time invariant filter. Most of the

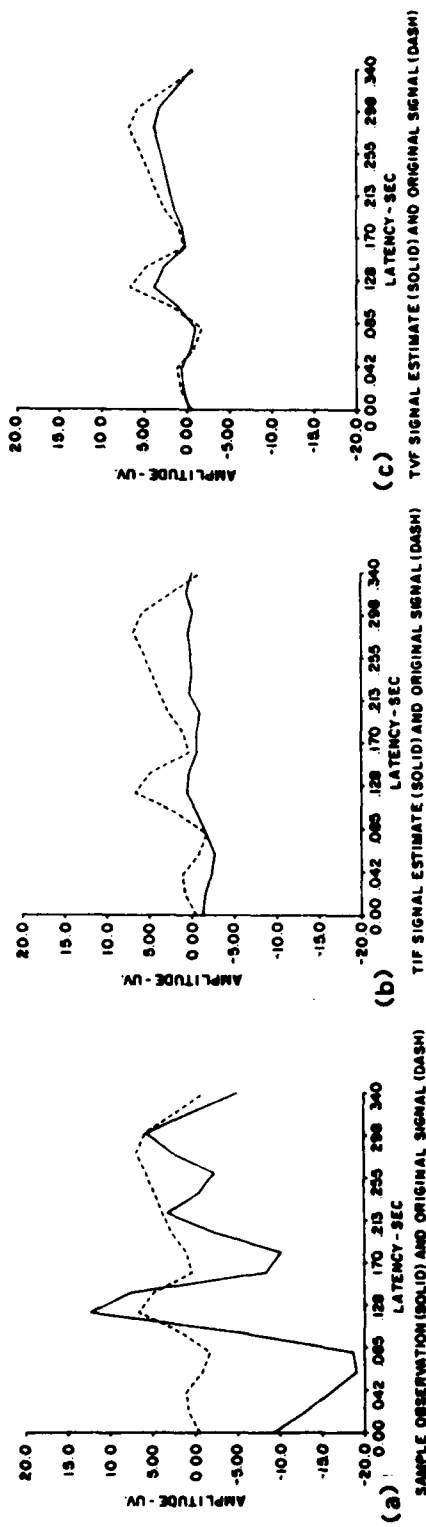


Fig. 3. Comparisons of Time Invariant and Time Varying Filter Performance (Sample No. 1).

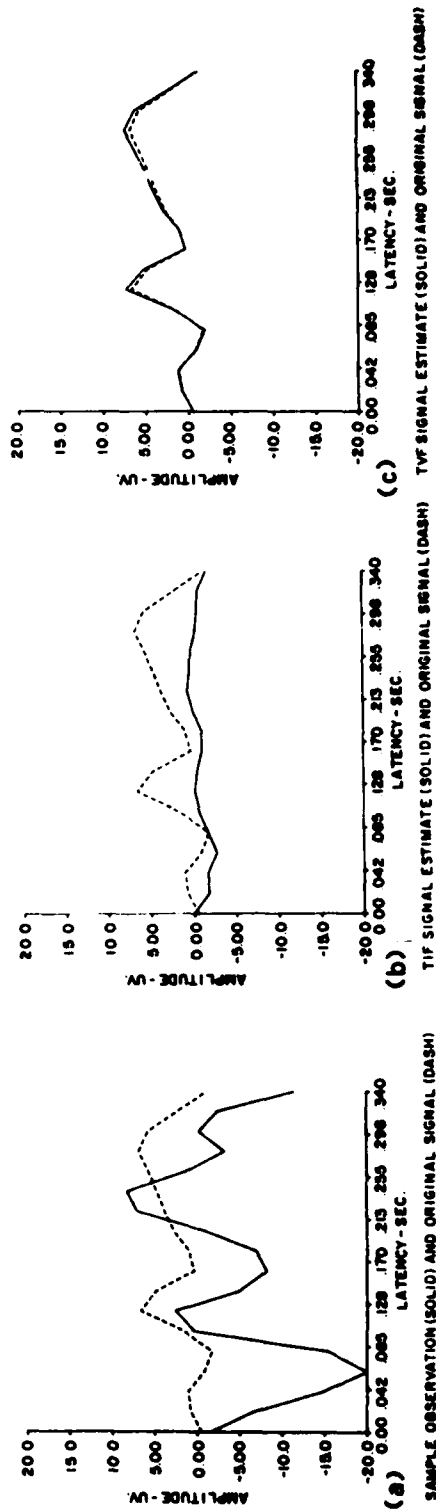


Fig. 4. Comparisons of Time Invariant and Time Varying Filter Performance (Sample No. 2).



noise is filtered out by the time varying filter.

The same set of data was used to evaluate the mean square error performance of the filters as a function of signal-to-noise ratio. The noise samples are scaled so as to provide the specified signal-to-noise ratio. For a signal-to-noise ratio typical of those occurring in evoked potential research (-10 dB), the mean square error was found to be 0.89 for time-invariant filter and 0.36 for time-varying filter.

The time varying filter adjusts to the transient nature of the signal and nonstationarity of the noise and provides a more powerful filtering operation than does the time-invariant filter. The time-invariant filter is only effective for stationary processes and thus cannot be expected to be optimum for ERP waveforms originating from an inherently nonstationary process.

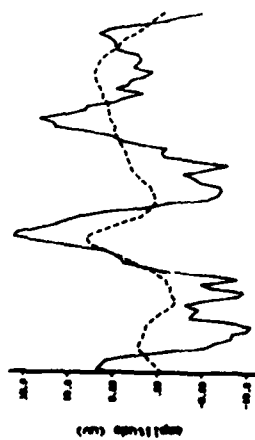
In order to demonstrate the performance of the filters in a realistic manner yet retain enough control of the test parameters to permit verification of the performance, signals were modified to simulate more realistic conditions. The noise was generated from random samples having a covariance matrix identical to that of experimentally measured samples of a human on-going EEG measured at scalp electrode position Pz. The basic signal was the same average evoked potential described previously. The signal was added to samples of the noise to give a signal-to-noise ratio of -6 dB. Jitter was produced by introducing random time delays in the signal employing a Gaussian distribution with zero mean and standard deviation 8 ms. This choice is justified by previous studies on typical evoked potential waveforms.

Two filters were designed to process the data records. One filter ignored the effects of signal time jitter and is called a constant latency filter while the other filter took this effect into account and is called a variable latency filter. In order to illustrate the noise cancelling performance of the filters, noise waveforms without the signal were processed as well as the signal plus noise waveforms. A sampling interval of 4 ms was employed.

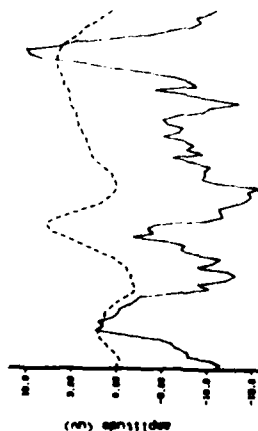
Fig. 5 shows results for signal latencies of 0, +12 and -12 ms. In this figure the left hand waveforms show the unfiltered signal plus noise (solid) and the underlying signal component (dashed). The center waveforms are the outputs of the constant latency filter (solid) and the true signal waveform (dashed). The right hand waveforms are the outputs for the variable latency filter (solid) and the true signal (dashed). It is evident from these waveforms that the filtering action of both filters is very strong and eliminates virtually all components not related to the signal waveform. The constant latency filter has the least error when no signal displacement is present. However, when signal displacement is present a better result is obtained with the variable latency filter. In particular, the locations of the peaks can be accurately recovered when the filter that incorporates the jitter effect is employed.

Fig. 6 shows the results of filtering the noise waveforms of Fig. 5, with no signal component present. In this figure the left hand waveforms are the noise waveform (dashed) and the filtered output (solid) for the constant latency filter and the right hand waveforms are for the variable latency filter. It is evident that strong noise suppression occurs when only noise is present.

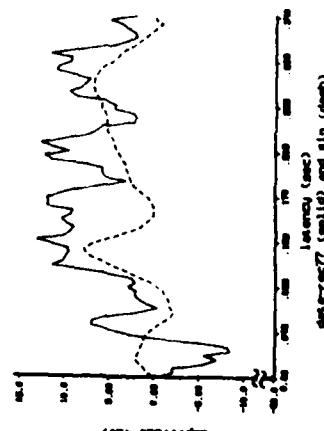
A more elaborate simulation which makes use of basis functions was carried out to illustrate the effectiveness of the time varying filter with more variable signals. The signal is composed of several signal components, each of which is allowed to move randomly and independently according to a Gaussian probability distribution. The desired signal components are typical of those found in evoked potential waveforms and are represented here by raised cosine wavelets. The polarities, latencies, amplitudes and the standard deviations of the latency jitter were obtained using the latency corrected averaging procedure and were used to estimate the covariance matrices required to design the filter. The basic components are illustrated in Fig. 7 in locations corresponding to zero latency jitter. Each component consists of a single loop of a cosine pulse having a duration of 40 ms.



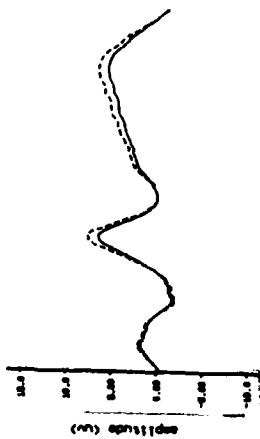
Signal plus noise.



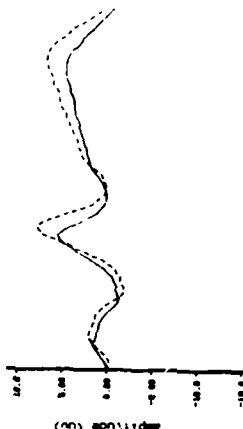
Signal plus noise.



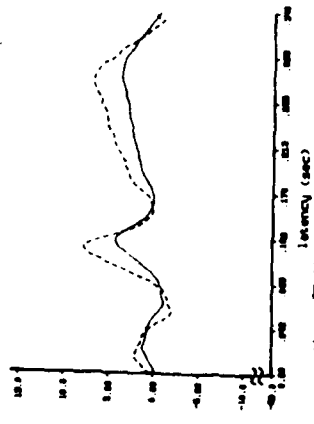
Signal plus noise.



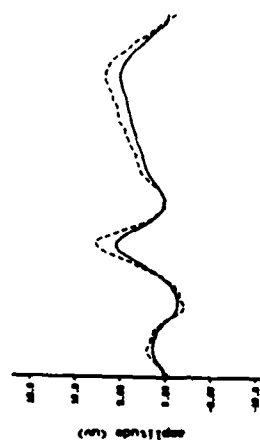
Constant latency filter output.  
(a) Signal without displacement.



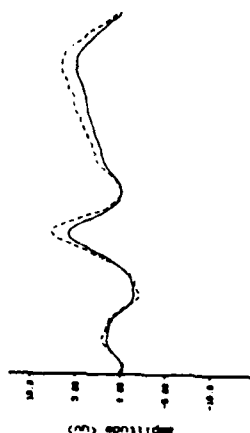
Constant latency filter output.  
(b) Signal with +12 ms displacement.



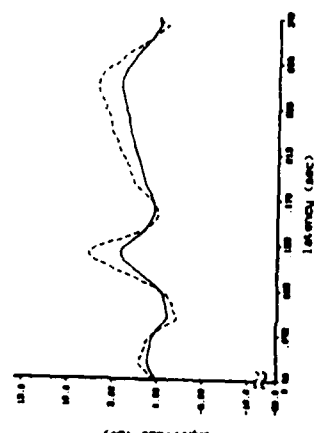
Constant latency filter output.  
(c) Signal with -12 ms displacement.



Variable latency filter output.



Variable latency filter output.



Variable latency filter output.

Fig. 5. Filtering of Signals with latency shifts (true signal shown dashed).

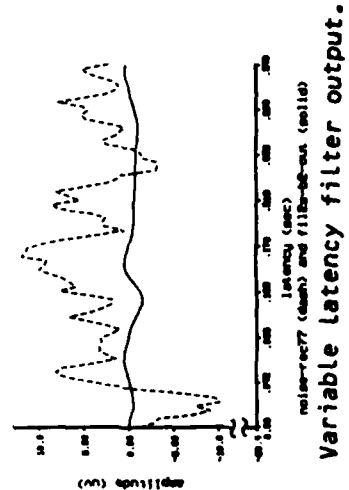
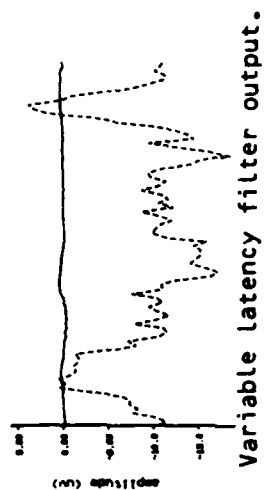
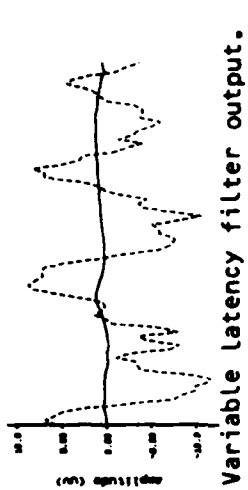
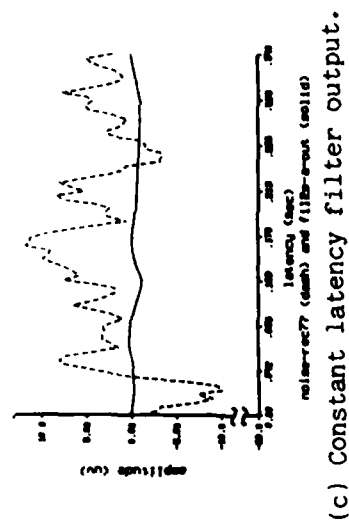
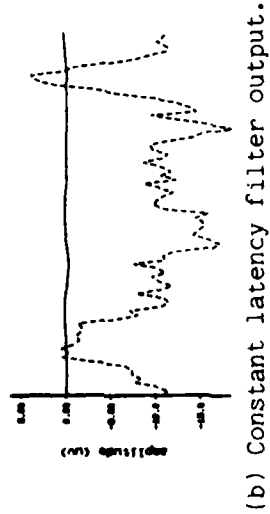
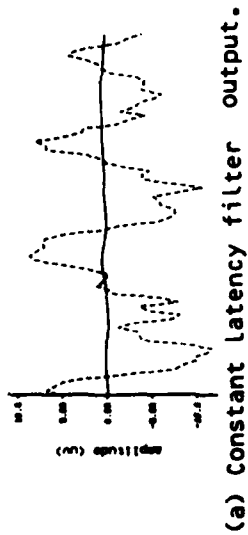


Fig. 6. Filtered noise waveforms of Fig. 5 with no signal present.

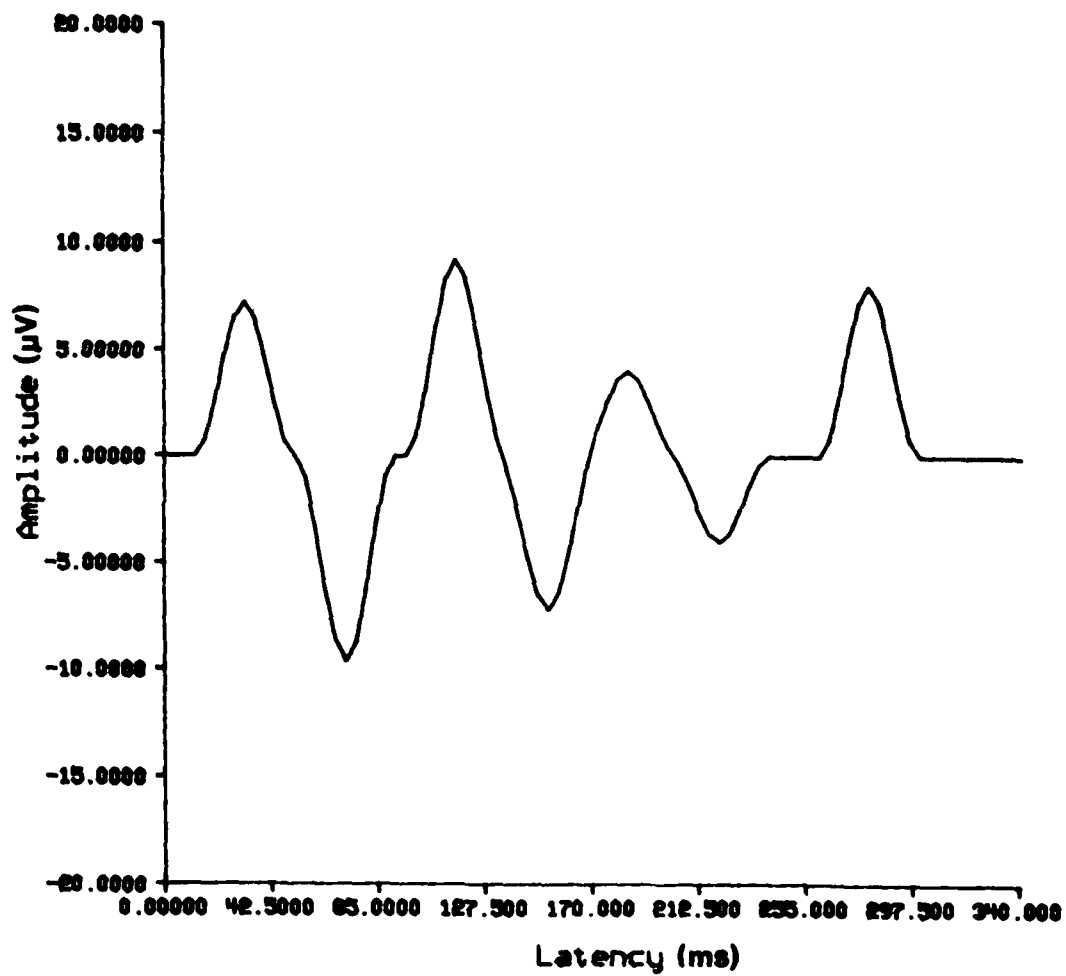


Fig. 7. Basis functions used for simulation of EP waveforms.

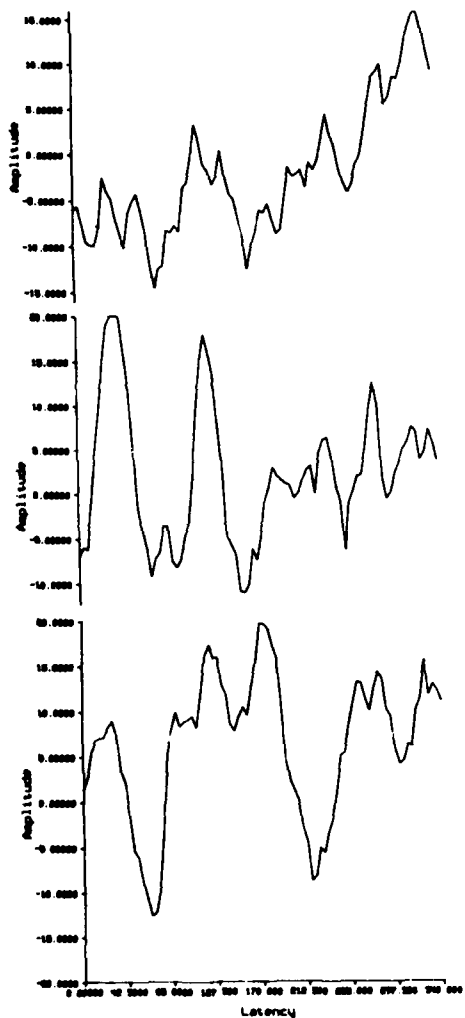
The noise was generated from random samples having a covariance matrix identical to that of experimentally measured EEG samples. The signal was randomly generated and consisted of the seven components described above. These randomly jittering components are added to the samples of the noise to provide a sample function of signal plus noise. The resulting data were then processed by the optimal time varying filter. Samples of the randomly generated signal were also processed by the filter to investigate the distortion performance when signal alone is present. In order to illustrate the noise cancelling performance of the filters, noise waveforms without the signal were also processed.

Fig. 8 shows samples of simulated signal plus noise and the corresponding filtered outputs. In this figure, the left hand waveforms show the simulated signal plus noise. The right hand waveforms are the outputs of the filter (solid) and the true underlying randomly generated signal (dashed). It is evident from these waveforms that the filter is very effective in eliminating virtually all components which are not related to any of the underlying components.

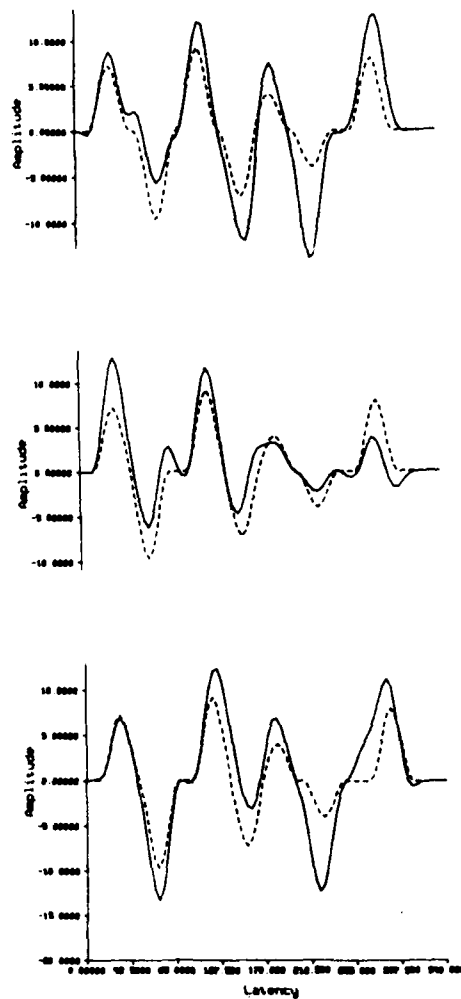
Fig. 9 shows the results of filtering the signal only and noise only corresponding to the waveforms of Fig. 8. In these figures the left hand waveforms are the signal waveform (dashed) and the filtered output (solid) and the right hand waveforms are the noise waveforms (dashed) and the filtered output (solid). It is evident that the signal passes through the filter with little distortion while the noise is substantially filtered out when processed by the filter.

#### Measurement of Detailed Structure of EP Waveforms

*Improved Instrumentation.* As part of the research program aimed at investigating the fine structure of EP waveforms it was found necessary to substantially modify the method of controlling the stimulus presentation so that uncertainties in the timing produced by the CRT could be eliminated from the experimental procedure.



(a) Samples of signal plus noise



(b) outputs of the filter (solid) and underlying signal (dash).

Fig. 8. Filtering of random latency signals plus noise with time-varying filter.

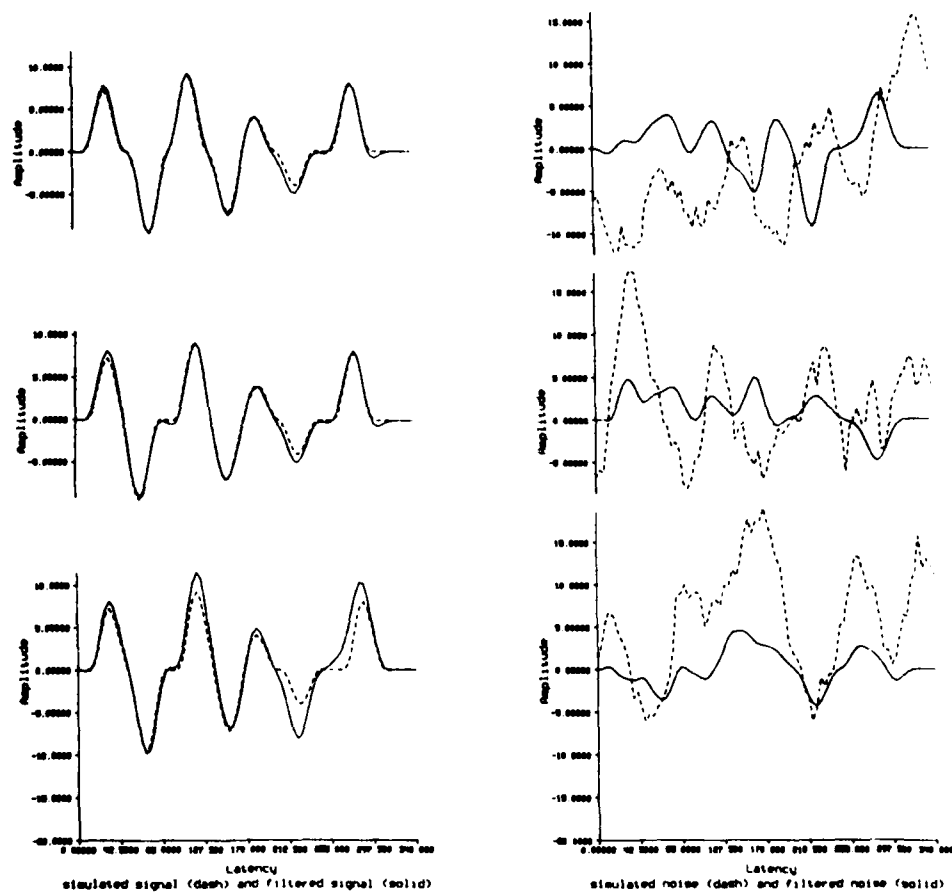


Fig. 9. Filtering of signal only and noise only for simulated data of Fig. 8.



In a raster scan display system, the image presented on the video monitor is swept out by a beam which begins in the upper left hand corner of the display and traces across the screen to the right and slightly down. This is repeated 262 times to trace out the entire field. Approximately 17 ms are required to trace out one field of an image. In most display systems the raster scan is synchronized to some periodic source and when a trigger is sent to initiate a stimulus presentation, unless the trigger is synchronized to the same source, there will be a random time variation between the time of the trigger and the time of the stimulus presentation. The uncertainty is greatest when stimulus occupies only a small fraction of the raster. Accurate synchronization of the EEG data sampling with the stimulus presentation will insure that the beginning of the tracing of the stimulus image on the video monitor occurs at the same sampling instant in each record. If data sampling is initiated at the time of stimulus presentation, then the vertical retrace pulse can be used as a fiducial point for synchronization with the data sampling. The stimulus image may cover only a portion of the field, in which case, following a vertical retrace, there is a time delay before the vertical scan begins tracing the top of the stimulus image. An appropriate time delay can be added after the vertical retrace before initiation of sampling so that the first sample value corresponds to the exact time of the beginning of image presentation.

It is often desirable to randomize the interstimulus interval and to initiate recording of data prior to stimulation. In this case the vertical retrace pulse cannot be directly used to initiate sampling. This is because there may not be an integer number of fields between the initial vertical retrace and the time of stimulus presentation. Without synchronization, the time at which the vertical scan begins tracing the top of the stimulus image is a random variable with respect to the sampling instants across the repetitions. This random variable is uniformly distributed over a 17 ms interval. It is possible that this random variable contributes to the latency jitter found in the individual components of the event related potential (ERP). The system described here

was developed to correct this problem by finding a method to synchronize the presentation of a visual stimulus with the data sampling. Synchronization is a desirable property of the stimulus for sharp, well-defined peaks to be found by averaging. Additional latency jitter due to stimulus presentation time jitter would make the average an even more unreliable estimate of the underlying signal.

By aligning a photodetector with the top of a block of light presented in the middle of the monitor and sampling its output as though running an experiment, it can be determined whether the stimulus is being presented at the same instant in each interval as portrayed in Figure 10. It was found that the photodetector output showed the appearance of the light source at random time samples which were uniformly distributed over a 17 ms interval. This result verified that the stimulus was not time-locked.

The first attempt to synchronize the presentation of the stimulus was hardware intensive. The tests were performed using visual stimuli generated by an IBM-PC computer and presented in the system monitor. The CRT controller for the IBM display is a Motorola 6845. According to Motorola documentation for this chip, the user should be able to reset all the counter registers by applying a negative pulse to the  $\overline{\text{RESET}}$  input on the chip. The advantage of using this method is that the raster scan can be reset to the top of the screen at any time and thus synchronized with the data sampling. This method requires some modification of the video display board to generate the appropriate reset signal with a software command. Unfortunately this attempt did not solve the problem. The Motorola documentation was apparently inaccurate in this instance and it was not possible to reset the CRT controller in this manner to synchronize the stimulus and data sampling.

A different approach was tried using both hardware and software. One input to the IBM control program is the prestimulus sampling interval (PSI), which is the amount of time during which the ongoing EEG is sampled before stimulation. Using this parameter, a delay time between a vertical sync pulse and the initiation of data

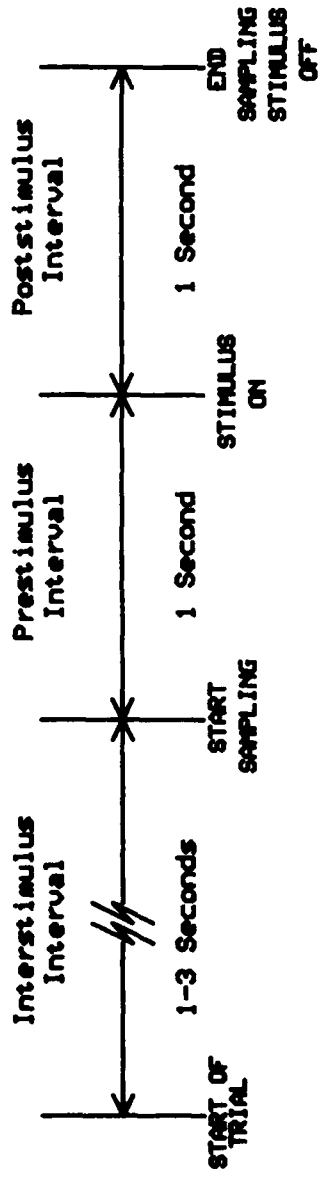


Figure 10. Timing Diagram for Stimulus Synchronization Test.

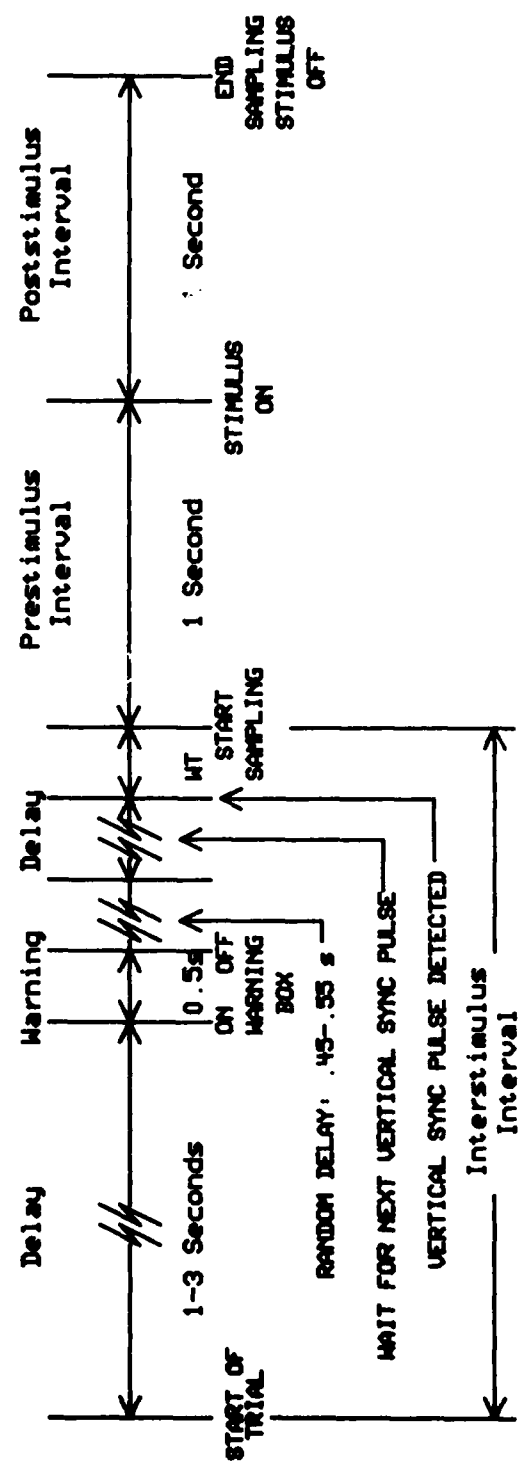


Figure 11. Timing Diagram for Sternberg Paradigm Experiment.

sampling can be computed. In addition, this delay time can be adjusted to account for the time required for the video scan to travel from the top of the monitor (which begins immediately following a vertical retrace) to the top of the stimulus figure. This additional time interval is referred to as the stimulus delay time (SDT).

Calculation of the total time delay is as follows:

$$\begin{aligned} WT &= VT - [PSI \bmod (VT)] + VT + SDT \\ &= VT \cdot \left[ 2 - \frac{PSI \bmod (VT)}{VT} \right] + SDT, \end{aligned}$$

where    WT    =    wait time after receiving vertical sync pulse,  
          VT    =    vertical field scan time = 16.6879 ms,  
          PSI    =    prestimulus sampling interval (ms),  
          SDT    =    stimulus delay time (ms).

The calculation of the stimulus delay time (SDT) is:

measure x = distance from top of display to top of image (inches).

$$SDT (ms) = \frac{x}{8.875} \cdot \frac{480}{524} \cdot (16.6879 \text{ ms}),$$

where            8.875            =    total screen height (inches),  
                  480                =    # of visible scan lines,  
                  524                =    # of total scan lines,  
                  16.6879 ms        =    vertical field scan time.

During the experiment when sampling is to be initiated, the program first waits for the appearance of a vertical sync pulse from the video controller. When this pulse is detected, the program waits the precomputed delay time (WT) and then initiates data sampling. The timing diagram for one trial of the experiment is shown in Figure 11.

It is necessary to detect the vertical sync pulse in order to begin the delay time. This was done by wiring the vertical sync pulse from the video board to one bit of the parallel I/O port. This bit is read constantly and its transition signals the appearance of a vertical sync pulse and the time delay (WT) is initiated.

The effectiveness of the synchronization procedure became immediately apparent in the conventional average EP computed from data measured with the modified systems. Figure 12 shows the average of 100 EP's resulting from application of visual stimuli that were small numbers centered on the face of the CRT. Because of the precise synchronization of the sampling to the stimulus presentation the electric fields radiated by the deflection circuit of the display are also synchronized. Because of this synchronization the electrical fields picked up by the wires from the scalp electrodes add coherently from one presentation to the next producing the noisy waveform shown in Figure 12. The problem was completely eliminated by moving the display monitor outside of the shielded test chamber and having the subject view the monitor through a glass window.

One of the purposes of increasing the precision of the timing measurement was to determine whether the randomness in the normal procedure was producing an increase in the random latency variations of the components in the individual EP's. Figures 13 and 14 show the histograms of component latencies for EP's obtained during the Sternberg paradigm experiment that is described in detail later in this report. Data for Figure 13 were measured before modification of the timing system, and data corresponding to Figure 14 were measured after the modification. It is evident from the figures that a better clustering of the latencies of peaks around this means occurs for the data

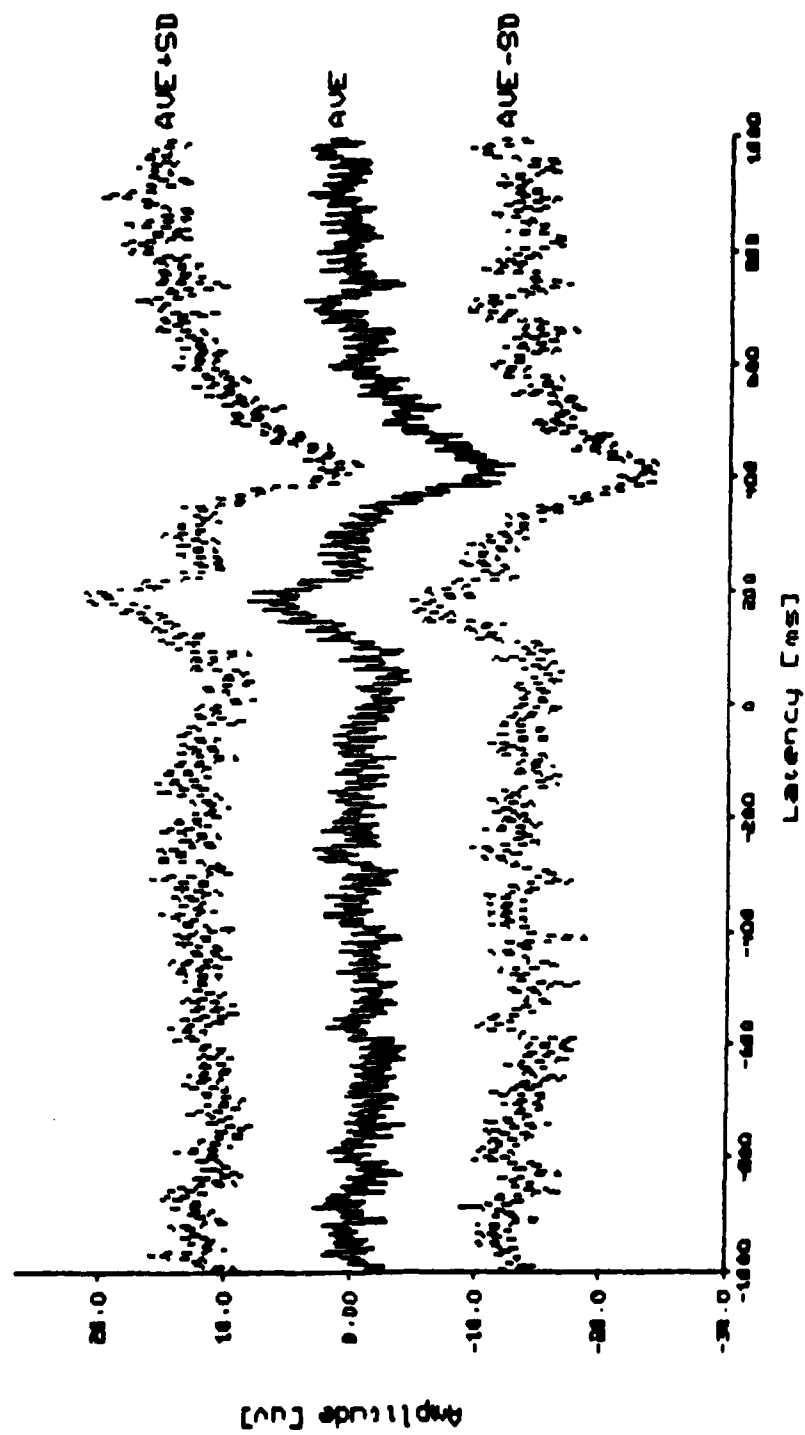


Figure 12. Average VEP showing coherent summation of pickup noise after timing modification.

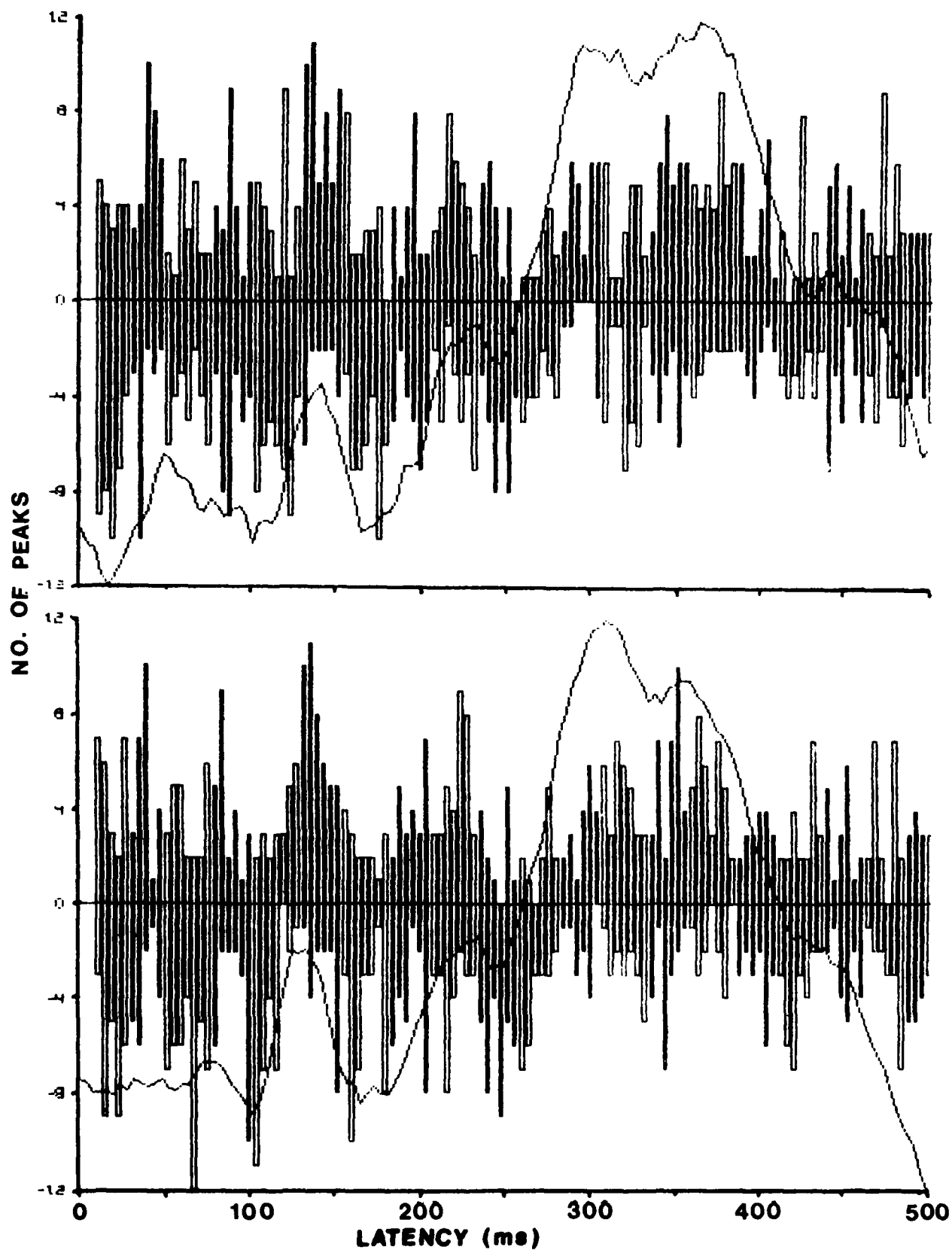


Figure 13. [Top] Histogram of VEP peak latencies before timing synchronization.

Figure 14. [Bottom] Histogram of VEP peak latencies after timing synchronization.

measured with the improved synchronization. This is most noticeable in components having latencies less than 300 ms. A precise determination of the reduction in jitter is very difficult to make because of the overlapping of the distributions. However, visual study of the histograms indicates that the reduction in the standard deviations is on the order of 2-3 ms. This leaves inherent random latency variations with standard deviations in the range of 7 ms or more still present in the individual EP's.

*Experimental Measurements.* The Sternberg paradigm was selected for generating experimental EP waveforms to be used in this research. The subjects in the experiments were instructed to respond to the visual presentation on a CRT of a single digit in one of 2 ways. A target button was to be pushed if the digit presented was in a previously memorized target set of digits. A different button was to be pressed in response to a digit which was not contained in the target set. The digits presented were 1 through 9. The number of digits in the target set was varied in different portions the experiment, being either 1, 3, or 5 target digits. Target set elements remain the same during the experiment. The sequence of presentations of target and non-target digits and the actual digit presented from the set were determined by the use of a random number generator internal to an IBM PC computer, which was used to generate and present the stimuli, control timing, and initiate data sampling. Digits from the target set occurred approximately 50% of the time.

Stimulation occurred in sessions of 60 at a time with a 2 to 5 minute rest period for the subject in between sessions. Twelve sessions of data taking were carried out. The order of the number of digits in the target set was 1, 3, 5, repeated 4 times. This provided in most cases sets of 100 usable data records for each number of target digits in the target and non-target response classes. Before each of the first 3 sessions, practice runs of 30 trials were given. Before each session, the target digits were reviewed with the subjects. The target and non-target response buttons were reversed midway through the experiment. A practice session of 30 responses was given before the session



following button reversal to accustom the subjects to the change. The button initially assigned as the target button was alternated across the subjects.

In some of the subjects tested, additional sets of sessions were added where the subject was instructed to respond only mentally, no button was to be pressed. A set of 3 sessions was added after the sixth session and another set of 3 sessions was added at the end of the normal sessions. These data were processed separately and will be analyzed at a later date.

Subjects in these experiments were college students or staff ranging in age from 23 to 31. They were comfortably seated in an IAC environmental chamber which has good sound isolating and electrical interference reducing qualities. The video monitor was placed outside the testing chamber to reduce AC interference, facing in through the chamber window at the subject's eye level, 1 meter from the eyes. A masking device on the window isolated external light from the chamber and allowed only a portion of the monitor to be viewed. The chamber was dimly lit by small incandescent light bulbs operating on DC power to prevent AC interference internal to the chamber.

The subjects were instructed to respond as quickly and consistently as possible without making a multitude of mistakes. They were instructed that 1 or 2 mistakes per session of 60 were tolerable. The index and middle finger of the right hand were used to respond. All subjects were right handed. The switches were low-force, positive action pushbuttons. An LED was dimly lit over the target button in case the subject needed a reminder during the session. The subjects were instructed to avoid eyeblinks and body movements between the time the warning box disappeared and the time they responded.

Data were recorded beginning 1 second prior to each stimulation and for 1 second after the onset of stimulation. The digit remained on for 1 second during which time the subject was to respond. Responses after this time were considered no-responses. The warning box was present for 1/2 second approximately 2 seconds before the onset

of stimulation. The time of presentation actually varied uniformly from 1.95 to 2.05 seconds to prevent alpha wave phase locking apparent in the averages of the responses as noted in pilot experiments. An interstimulus interval varying uniformly between 1 and 3 seconds occurred between the turning off of the stimulus and the onset of the warning box.

The warning box was a 0.5 cm square outline of a box centered on the monitor. The digits filled a rectangle 1.5 cm wide  $\times$  2.5 cm high centered on the monitor. The brightness was set fairly low to avoid noticeable persistence after the turning off of the figures and to reduce subject eye fatigue.

Beckman Ag-Ag Cl electrodes were applied to the scalp with double-sided adhesive collars and electrolyte cream at sites Oz, Pz, Cz, Fz, P<sub>3</sub>, and P<sub>4</sub> according to the 10-20 system. Reference was electrically linked ears. The electro-oculogram (EOG) was recorded diagonally across the left eye socket for detection of eyeblink and eye movement artifacts. A forehead ground electrode was attached. Electrode impedances were 10K $\Omega$  or below; in most cases these were below 5K $\Omega$ . Electrode impedances were tested after every 2 to 4 sessions and electrodes replaced if impedances had significantly increased.

The signals and response switchbox output were amplified by Grass 7P511 amplifiers with bandwidth set to 0.1 Hz to 100 Hz (3db bandwidth cutoff points). Data were monitored at the outputs of the amplifiers by a chart recorder and LED meters which indicated signal strength in 3db steps with the highest level corresponding to the  $\pm 1.0V$  range of the analog to digital (A/D) converter. Amplifier gain levels were adjusted to use the entire dynamic range of the A/D converter without saturation. The system was calibrated prior to the start of data recording.

The analog data were digitized by the LPS-11 laboratory peripheral system under control of a DEC PDP 11/45 computer with a UNIX operating system. The data were sampled at 250 samples per second and quantized to 12 bits. The raw data were

recorded on magnetic tape. Sampling was initiated by the IBM computer and was synchronized to the exact time of stimulus presentation (which occurred 1 second after sampling began). This synchronization process is discussed separately.

The data were then processed to detect eyeblink artifacts and A/D converter saturation. Any eyeblink detected or saturation occurring in any electrode data between 500 ms prior to and 400 ms after stimulation were rejected from subsequent processing. Eyeblink detection occurred when there was at least a  $50 \mu\text{V}$  change in 100 ms. Saturation occurred when 2 consecutive A/D limit values were detected. The first 3 records from each session were automatically rejected. The data were separated into files of 'n' or 't' for non-target or target digits, and 1, 3, or 5 for the number of digits in the target set. The files were then processed to separate the incorrect from the correct responses as determined by the response switchbox data. Statistics of the response times were computed.

Data files with correct responses only were averaged across the ensemble of responses for each class of data. Also, the variances of the averages were computed. Three sets of plots were produced for each electrode:

- 1) Average, average +1 SD, average -1 SD for each of the classes. Entire 2 seconds of data were plotted.
- 2) Averages for 1, 3, and 5 digits in the target set were plotted on the same graph for the target and non-target classes. 600 ms of data were plotted starting at stimulation.
- 3) Averages for target and non-target were plotted on the same graph for each of the various numbers of digits in the target set. 600 ms of data were plotted starting at stimulation.

Data files were produced which contained the segments of data from 0 to 600 ms. These data files for electrode Pz were then processed by the latency-corrected average (LCA) program. The statistics of the detected peaks were printed out. The histogram

of the detected peaks across the records along with the average were plotted. Peak detection was performed after the data was filtered by a MMSE filter and low-passed filtered to 25 Hz to smooth the data. The continuous latency-corrected average was computed for electrode Pz using the results of the LCA. These were plotted along with their corresponding averages.

A preliminary analysis of the Sternberg paradigm data has been carried out along the following lines.

- 1) The single ERP during a task relevant/irrelevant type of paradigm is composed of a series of peaks which may or not be related to the decision making process. The relationship that these peaks have to the decision making process was investigated in a Sternberg type paradigm designed to elicit a variety of responses under different experimental conditions.
- 2) It has been theorized that the P300 wave characteristic of this type of experiment is composed of a number of separate peaks which are "smeared out" during the conventional ensemble averaging process. Procedures such as the Latency Corrected Average (LCA) and the Continuous Latency Corrected Average (CLCA) were utilized with the data obtained from the experiments carried out in our laboratory. These techniques identify the individual components of a response permitting their correlation with other experimental variables to be determined.
- 3) Components of the event related potential other than P300 may be reliably correlated with the cognitive processing of data. This is an area that was investigated using the results of the LCA and the CLCA algorithms.

The results of the preliminary analysis are presented in two parts. First, an analysis is made of the average event related potentials obtained using the Sternberg paradigm described earlier. General characteristics of each of the responses is detailed and compared to the responses obtained from all of the electrodes used. Second, an

analysis is made of the LCA and CLCA results obtained for the experimental conditions.

Data for four subjects are shown in Figures 15-22. Figures 15, 17, 19, 21 correspond to averages for subjects 1, 2, 3, and 4 from four electrodes for responses when the stimulus contained a member of the target set. Figures 16, 18, 20 and 22 are averages from the same subjects for responses when the stimulus was not a member of the target set.

Subject #1 - (see Figures 15 and 16). The P300 wave occurred earlier in the target set than in the non-target set. This difference was of the order of 50 ms. In the target set, P300 for the one digit target set occurred at 360 ms whereas in the non-target set, it occurred at 410 ms. The separation in the latency of P300 for the different responses and for increasing numbers in the set was maintained in the event related potentials for the non-target set. The ERP's for the target set did not maintain this separation when the set size was increased from 1 to 3 to 5 numbers.

The P300 wave in both of the target and non-target ERP's is an easily identifiable low-frequency waveform. In the ERP's of the non-target set it is consistently preceded by a negative waveform at a latency of approximately 280 ms. For the target set, however, this negative waveform does not appear for the set size of one digit, and it is clearly visible for increasing numbers in the set.

The latencies of P300 in the Cz electrode were as follows:

ERP's for the Target Set:	1 number - 360 ms
	3 numbers - 405 ms
	5 numbers - 405 ms
ERP's for the Non-target Set:	1 number - 410 ms
	3 numbers - 450 ms
	5 numbers - 475 ms

Subject #2 - (see Figures 17 and 18) - As with Subject #1, the P300 wave occurred earlier in the ERP's for the target responses than for the non-target responses. The difference was on the order of 90 ms. In this subject, the P300 type activity seems to be a very low frequency phenomenon and thus it becomes difficult to distinguish whether any separation occurs for the P300 waveforms of the different set sizes. An indication may be obtained from the rising slope of the P300 wave, especially in the non-target ERP's, which indicate that indeed the 1,3 and 5 sets are separable by these ERP's (see Figure 18). Using the same method, however, it was not possible to demonstrate conclusively that the ERP's corresponding to the target set could be used to distinguish between the different sets.

Subject #3 - (see Figures 19 and 20) - The latency of the P300 waveform for the set size of one number occurs earlier in the target set than in the non-target set. This seems to be a consistent result with this subject and with previous subjects in the study. As with the preceding subject, the P300 phenomenon is of very low frequency and difficult to identify clearly. It seems as if there is a general trend to longer latencies with increasing set size, but this is only a subjective assessment of the data, since it is impossible to visually distinguish the different peaks. (See Figure 19).

Subject #4 - (see Figures 21 and 22) - The target ERP's for this subject show the characteristic earlier occurrence of P300 when compared to the non-target set. Although it is difficult to interpret the data because of the occurrence of multiple peaks in the P300 region, it seems as if the P300 waves corresponding to the higher order numbers in the set occur at longer latencies (see Figure 21). The non-target ERP's are even more difficult to analyze because of the lack of definition of the response in the P300 interval. By using the rising slope criterion on the target set of ERP's one could conclude that the P300 waves have increasingly longer latency for larger numbers in the target set (see Figure 22).

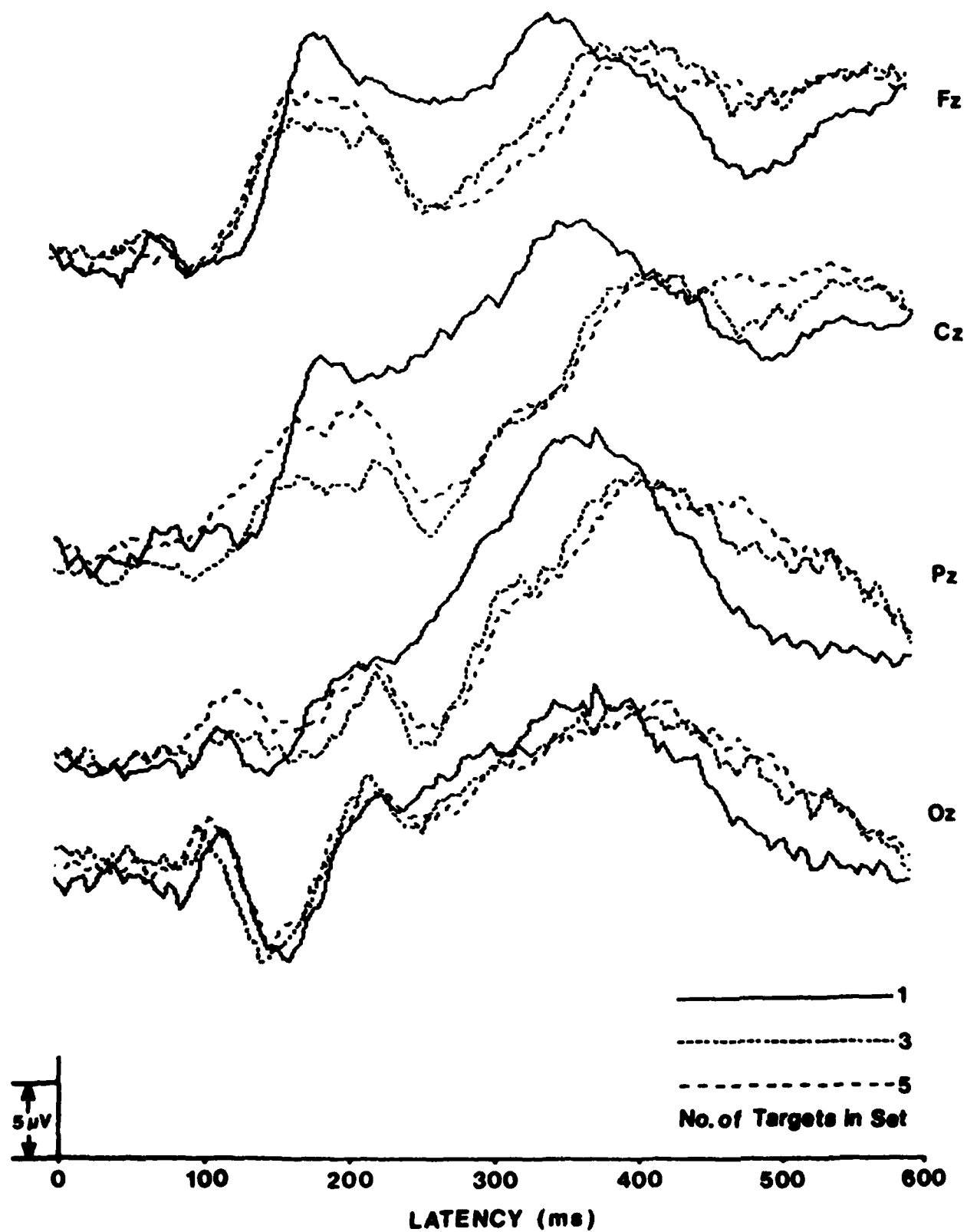


Figure 15. Conventional average for Sternberg paradigm.  
Target set. Subject 1

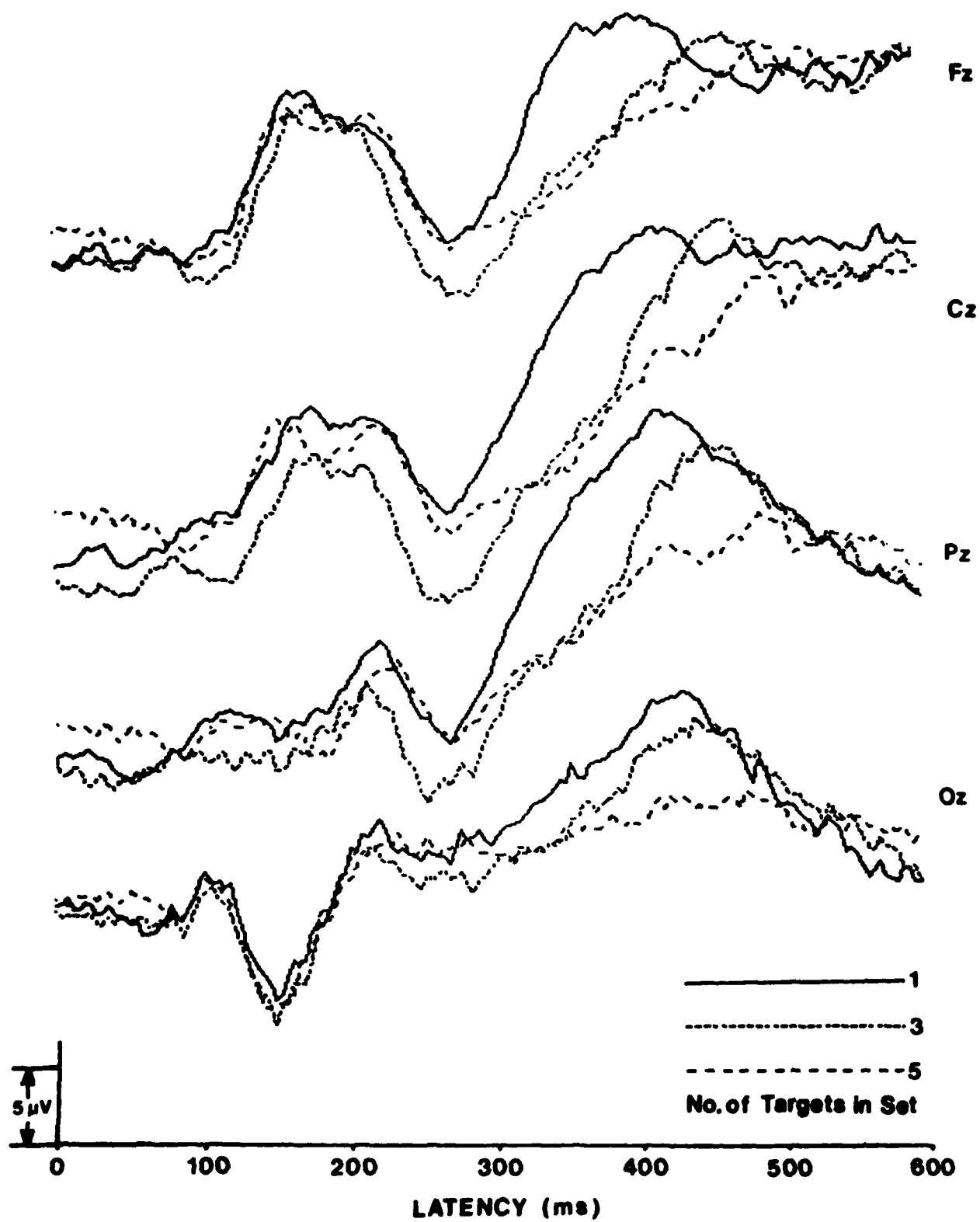


Figure 16. Conventional average for Sternberg paradigm.  
Non-target set. Subject 1



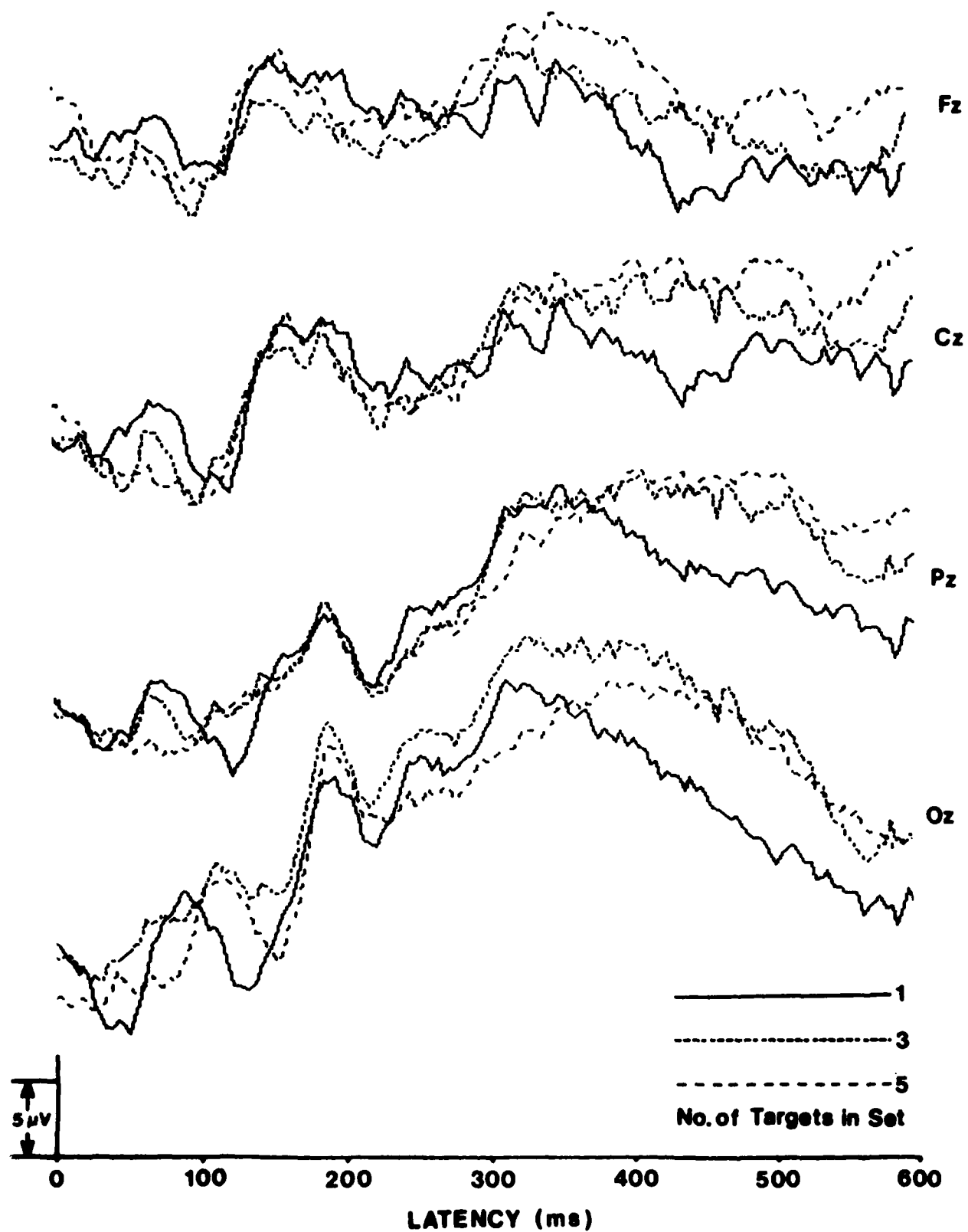


Figure 17. Conventional average for Sternberg paradigm.  
Target set. Subject 2

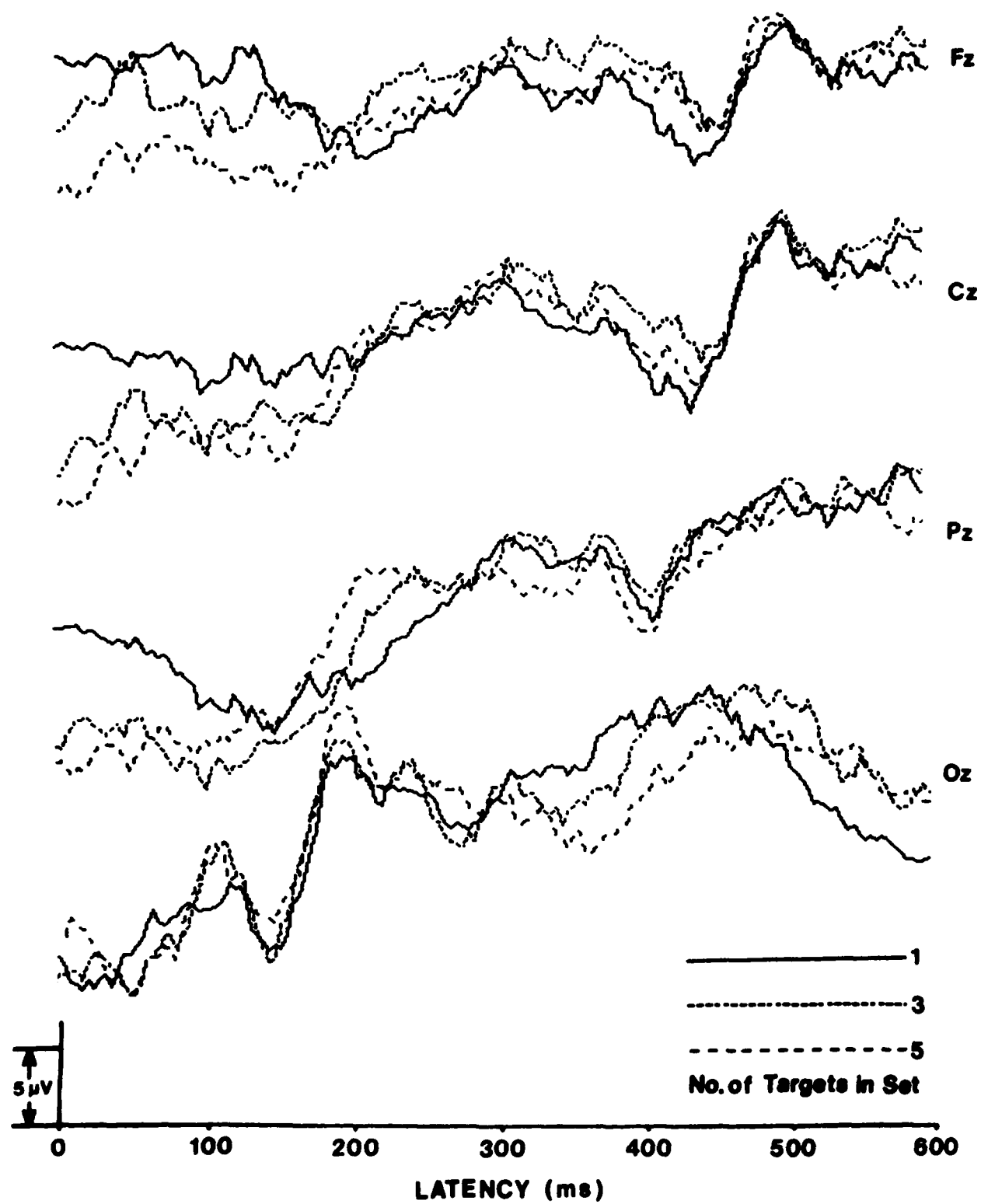


Figure 18. Conventional average for Sternberg paradigm.  
Non-target set. Subject 2

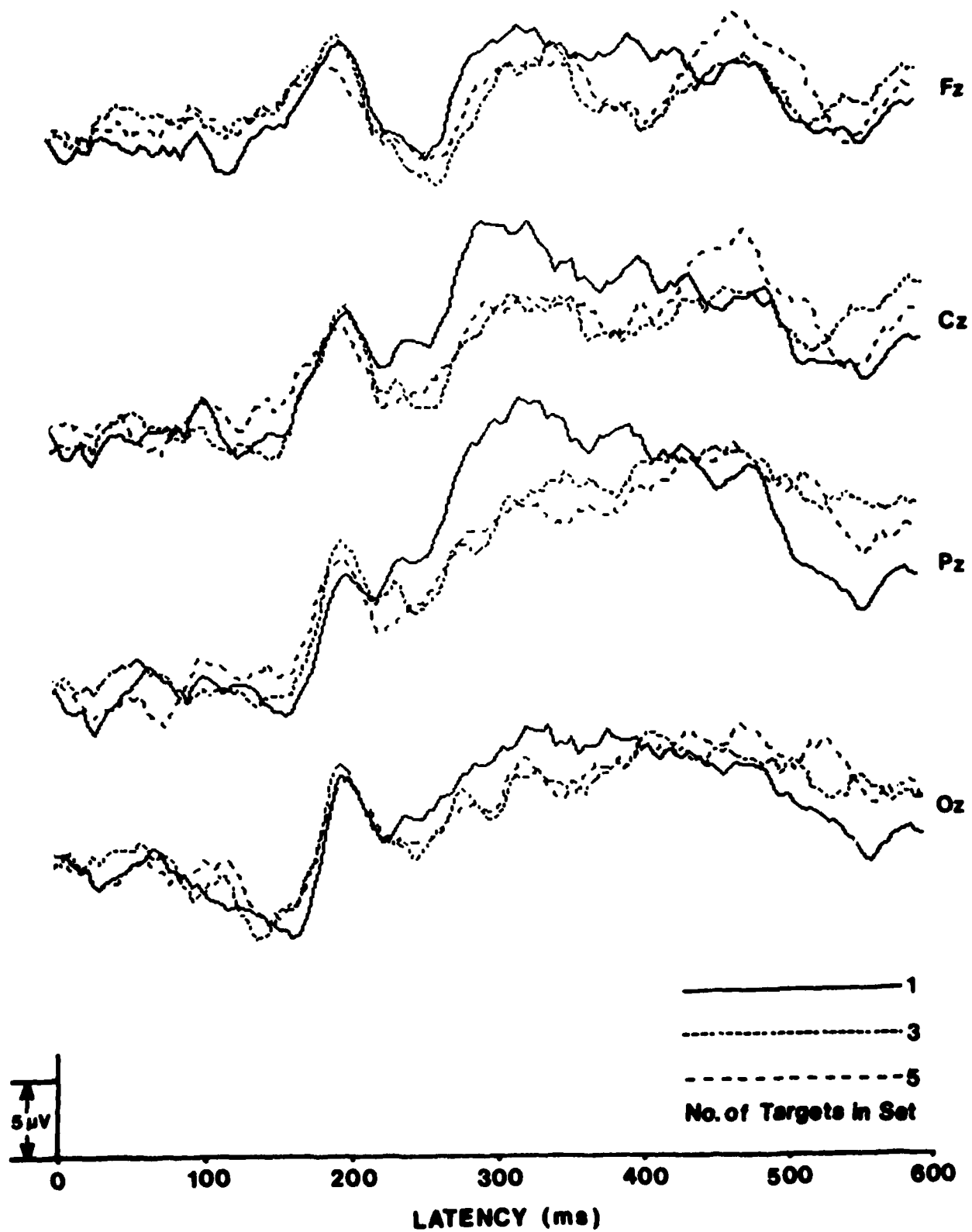


Figure 19. Conventional average for Sternberg paradigm.  
Target set. Subject 3

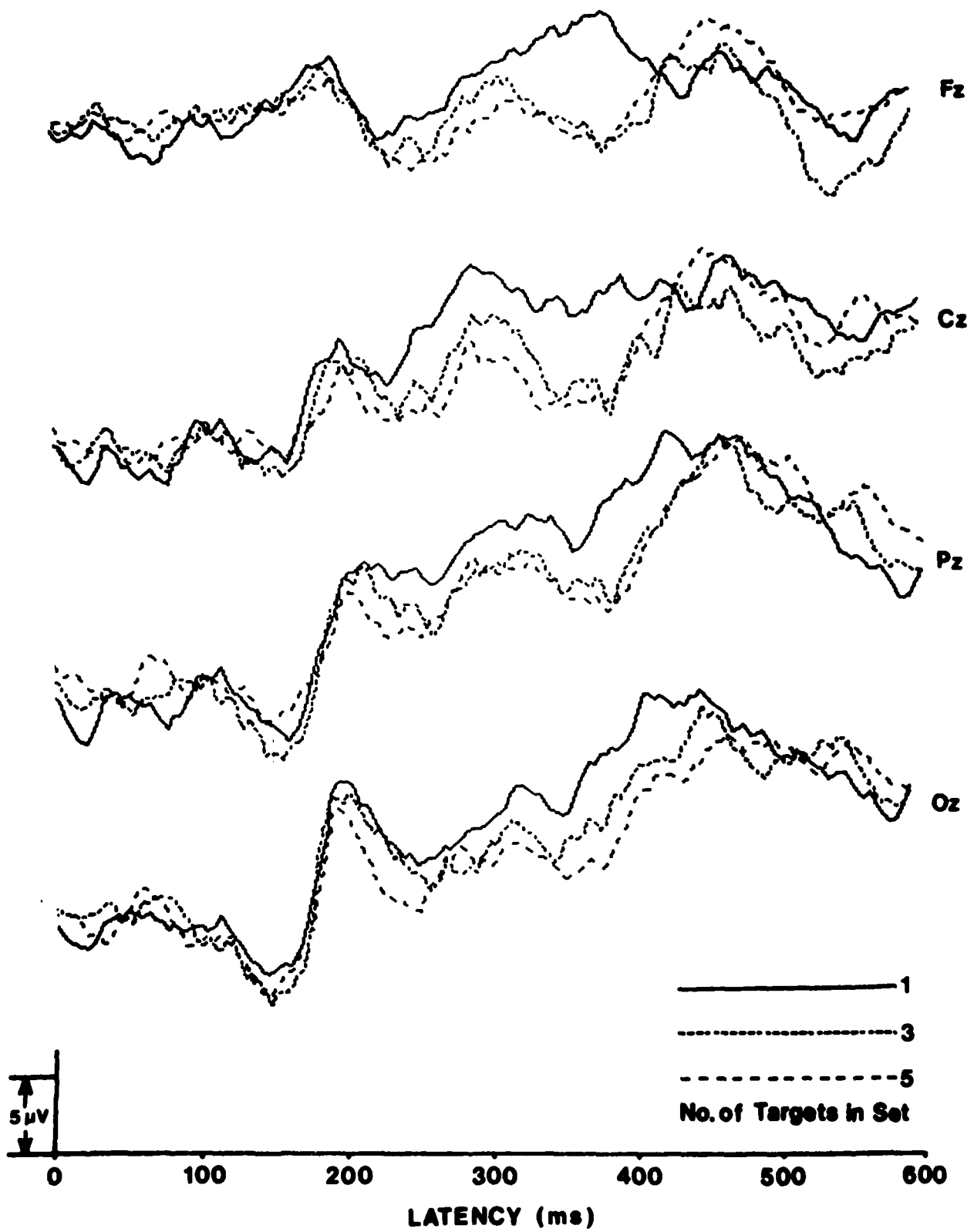


Figure 20. Conventional average for Sternberg paradigm.  
Non-target set. Subject 3

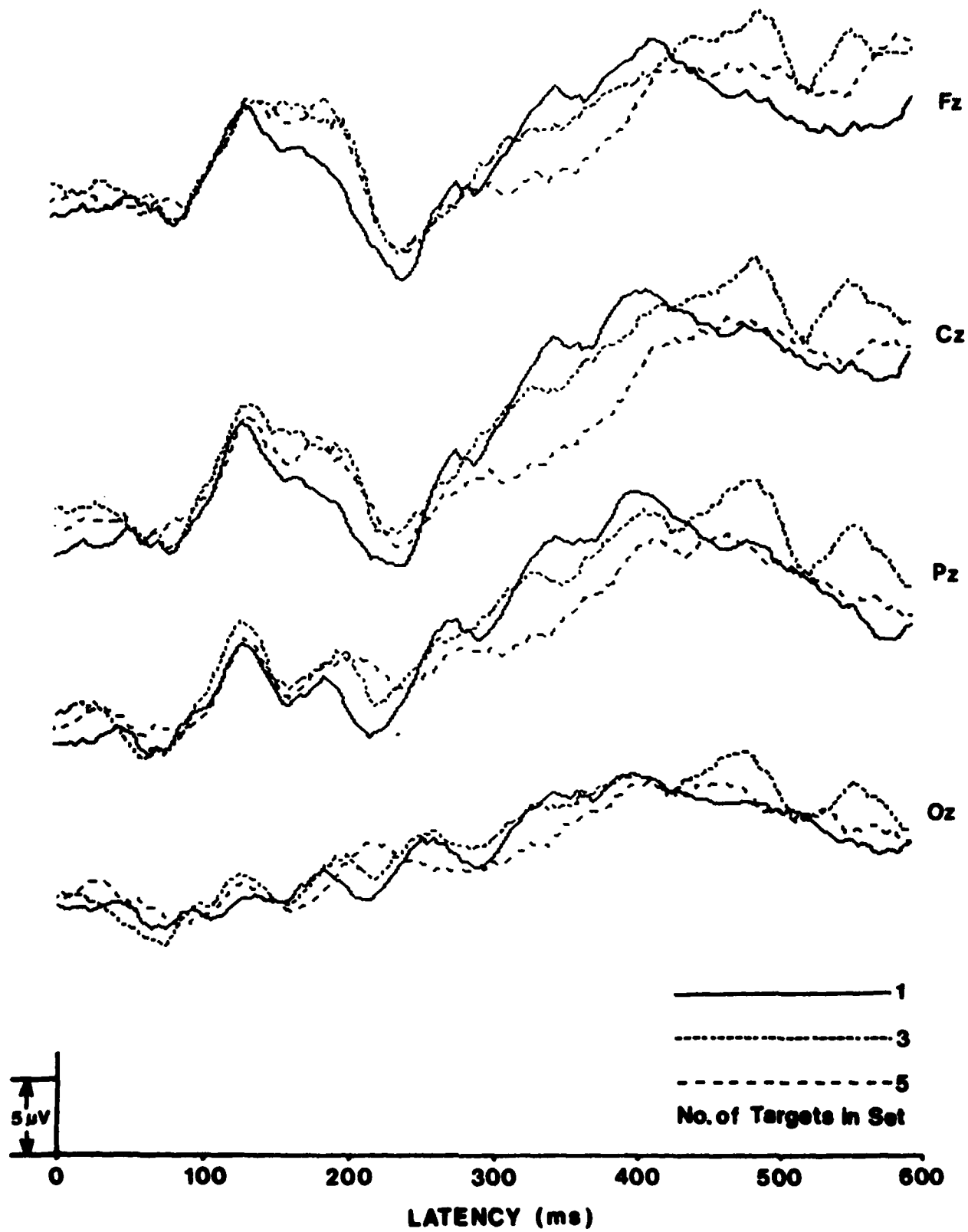


Figure 21. Conventional average for Sternberg paradigm.  
Target set. Subject 4

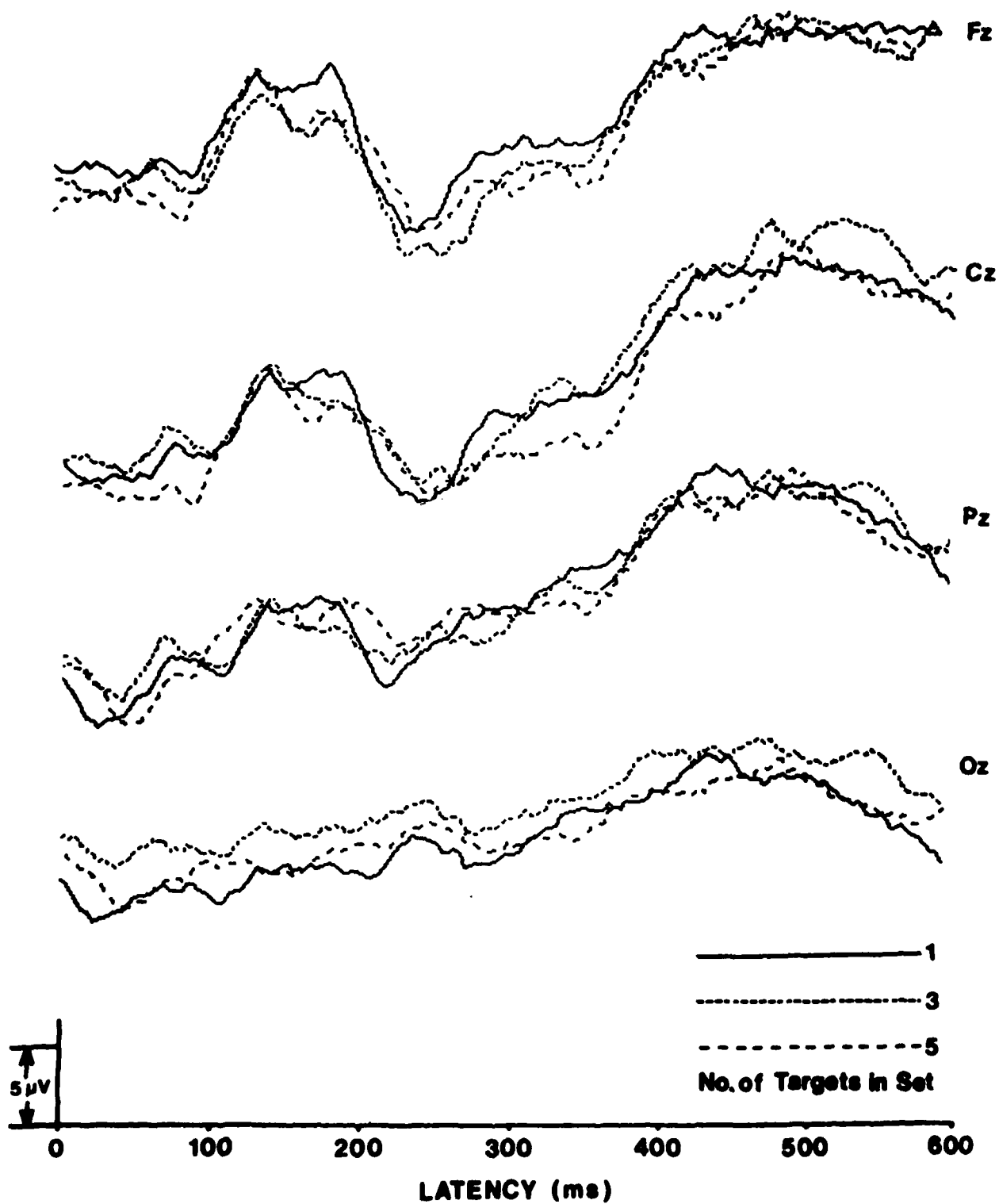


Figure 22. Conventional average for Sternberg paradigm.  
Non-target set. Subject 4

The structure of the ERP's was further analyzed by utilizing the results from the Continuous Latency Corrected Average (CLCA). Figures 23-30 are the Continuous Latency Corrected Averages (CLCA) for electrode Pz for the same test conditions as Figures 15-22. The solid line is the CLCA data and the broken line is the conventional average. Numerical results of the LCA procedure corresponding to these figures are given in the Appendix.

Subject #1 - (see Figures 23 and 24) - The results of the CLCA for this subject reveal an apparent substructure to the P300 waveform not shown in the conventional average response. It should be noted that if two consecutive peaks of the same polarity are found, the fitting procedure used by the CLCA interpolates and locates a peak of opposite polarity between them. Because of this, there are some peaks in the response that are artificial. The validity of any peak can be checked by the LCA tabular data given in the Appendix. The ERP's for the target response to one number show two positive peaks: one located at 347 ms and the other at 397 ms. For the three number set, there is one prominent positive peak, located at 393 ms. For the five number set, there is one prominent peak located at 401 ms. It is also noticed that whereas the peaks for the one and three number set are sharply defined, the one for the five number set is not. This kind of substructure of the P300 region is not readily recognizable from examination of the conventionally averaged ERP's of this data.

For the non-target set, a similar kind of substructure is demonstrated for the ERP's in the area of the P300 response. For the one number set, a series of three peaks are evident at latencies of 370 ms, 418 ms, and 451 ms. There is also a peak at 370 ms which is not immediately observed in the ERP's to the target set. For the three number set, the substructure is more evident, with positive paks at 376 ms, 414 ms, and 464 ms. For the five number set, although the procedure did not find a positive peak in the 370 ms area, the interpolating procedure located a peak there following the general pattern of the rest of the components of the response. The conclusion was

reached from examination of the averaged data that the non-target set showed an increase in P300 latency with an increase in the number of digits in the set. It is more difficult to arrive at the same conclusion from careful examination of the CLCA data. The data substructure appears to be composed of peaks that are consistently found in the CLCA but not found in the averaged data (see the peak found at 370 ms in the non-target set).

Subject #2 - (see Figures 25 and 26) - Analysis of the structure of the CLCA for the non-target set, reveals some interesting facts. There is a negative peak identified by the CLCA for the non-target set for the three and five number set respectively. This peak was not identified for the one number set perhaps because it was too low in the noise. Interestingly, the percent of the time that this peak is found appears to increase with an increase in the number of digits in the set. If one assumes that in the one digit case the peak was not found, in the three number set, it was found in 39% of the cases and in the five number case in 56% of the cases, then perhaps this peak might be associated (for the non-target case) with an increase in the number of digits in the set. It is also interesting to observe that, as with the first subject, this peak is not present in the ERP's corresponding to the target number being present.

The ERP's corresponding to digits in the target set have an increase in energy in the region between 300 and 400 ms which is not present in the non-target set ERP's. Using the previously described slope criterion for the activity in this region, one could conclude that the latency of the beginning of the activity in this region is directly related to the number of digits in the target set. The more numbers in the target set, the later the activity begins in this region. It still becomes difficult to associate an individual peak with the "P300" wave.

Subject #3 - (see Figures 27 and 28) - Analysis of the structure of the CLCA for the non-target set reveals again the appearance of a negative peak occurring between 360 ms and 390 ms. This peak is not readily identifiable in the average response. The



positive set for the three digits response also shows a negative peak occurring at approximately 397 ms. However this peak is not present in the response for the one digit and the five digit ERP. The area of the P300 response shows a structure which is difficult to interpret on the basis of the data for this one subject. It appears as if in the target ERP for the one digit set, the structure of the P300 response consists of a series of positive and negative peaks in the area between 300 and 400 ms. This same pattern of alternating polarity peaks seems to be present in the area following 400 ms in the ERP's for the non-target set corresponding to one digit.

Subject #4 - (see Figures 29 and 30) - The negative peak, characteristic of the non-target set of responses, is present in this set of ERP's. It is also present in the target set of ERP's but not as often. This suggests that this peak is of much lower signal-to-noise ratio in the target set of ERP's than in the non-target set of ERP's. This set of responses is also difficult to analyze because of the complex wave structure around the P300 interval.

Figures 31 to 34 show the superimposed CLCA plots for the target and non-target set of ERP's for the four subjects tested. Comparing these figures to Figures 15 through 22 where the conventional averaged ERP's were superimposed, it is observed that the P300 region exhibits a fine structure which is not readily discernible from the averaged ERP's. These very preliminary results indicated that the P300 phenomenon is not composed solely of a low frequency wave, but that a much finer structure and detail are the predominant characteristics of the endogenous response.

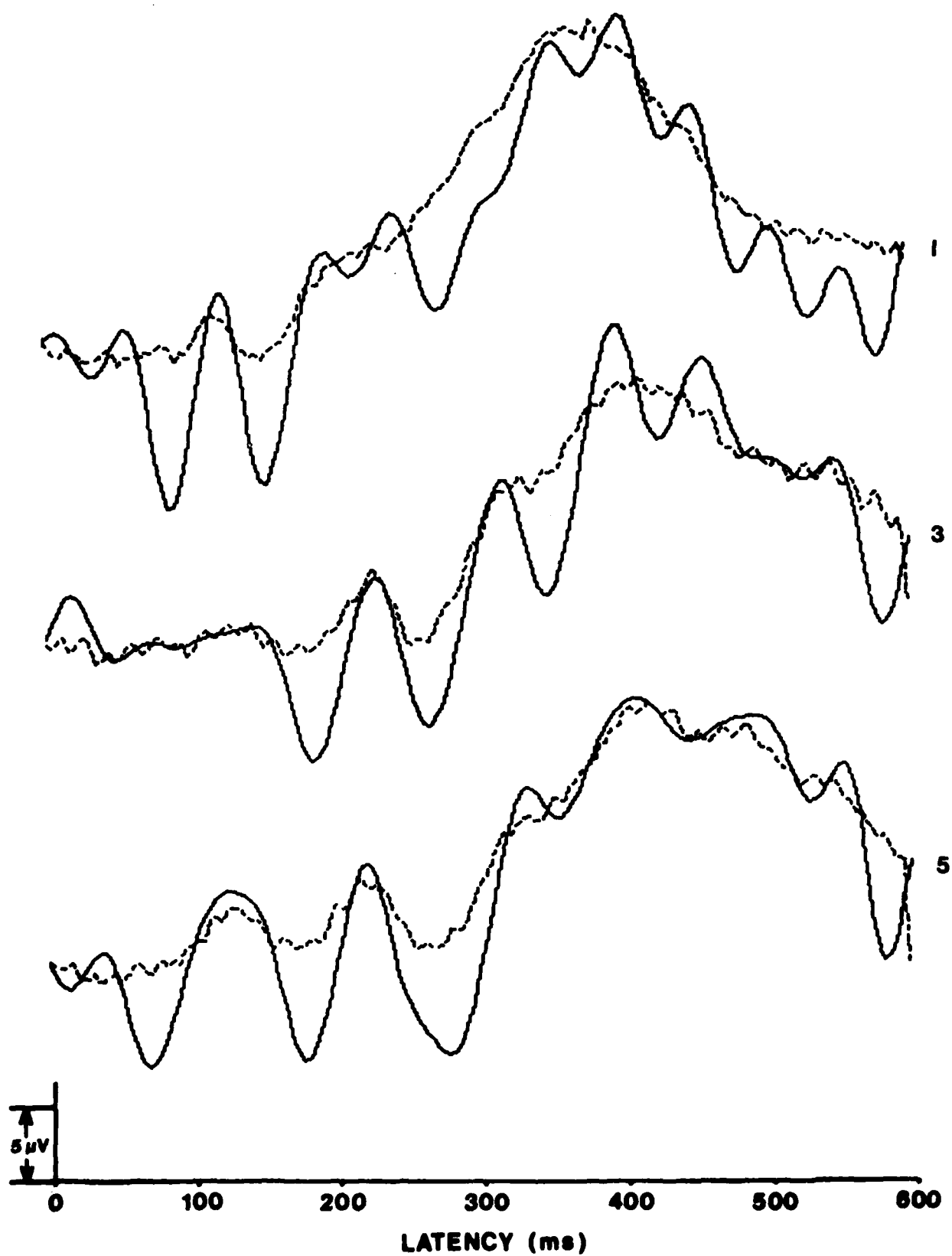


Figure 23. Continuous Latency Corrected Average (solid) and conventional average (broken) for Subject 1, target set. The number of targets in the set is indicated on the right.

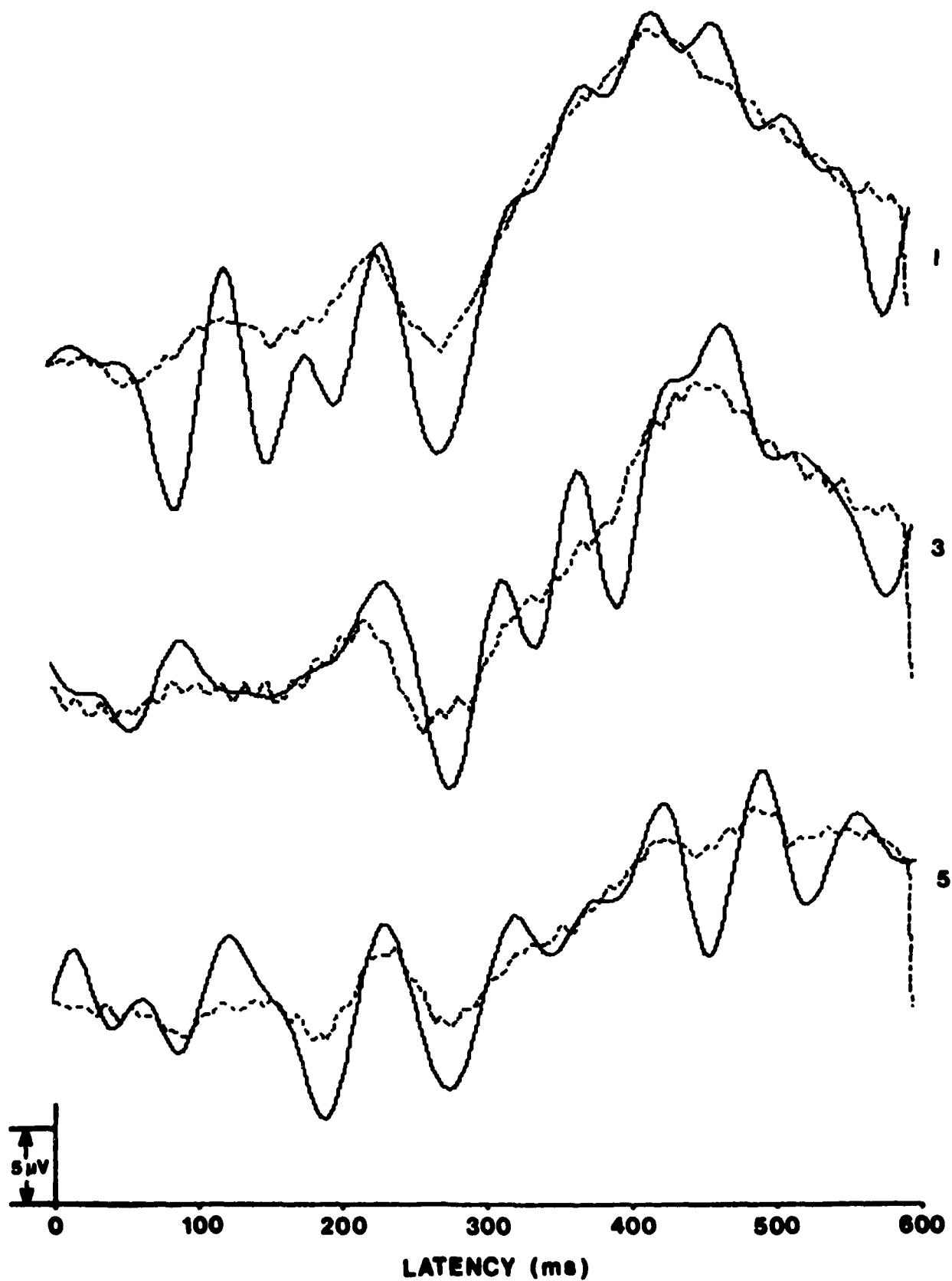


Figure 24. Continuous Latency Corrected Average (solid) and conventional average (broken) for Subject 1, non-target set. The number of targets in the set is indicated on the right.

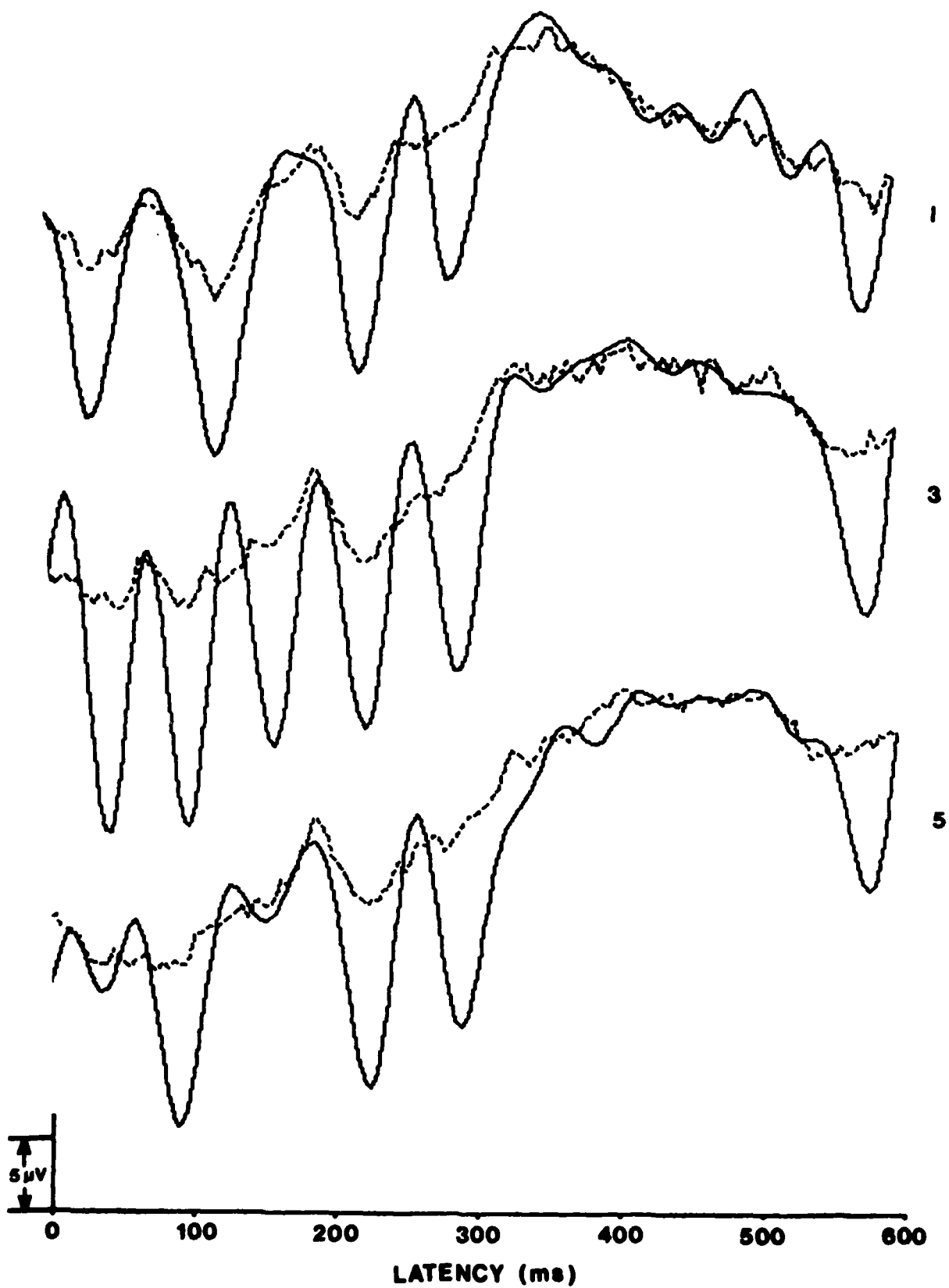


Figure 25. Continuous Latency Corrected Average (solid) and conventional average (broken) for Subject 2, target set. The number of targets in the set is indicated on the right.

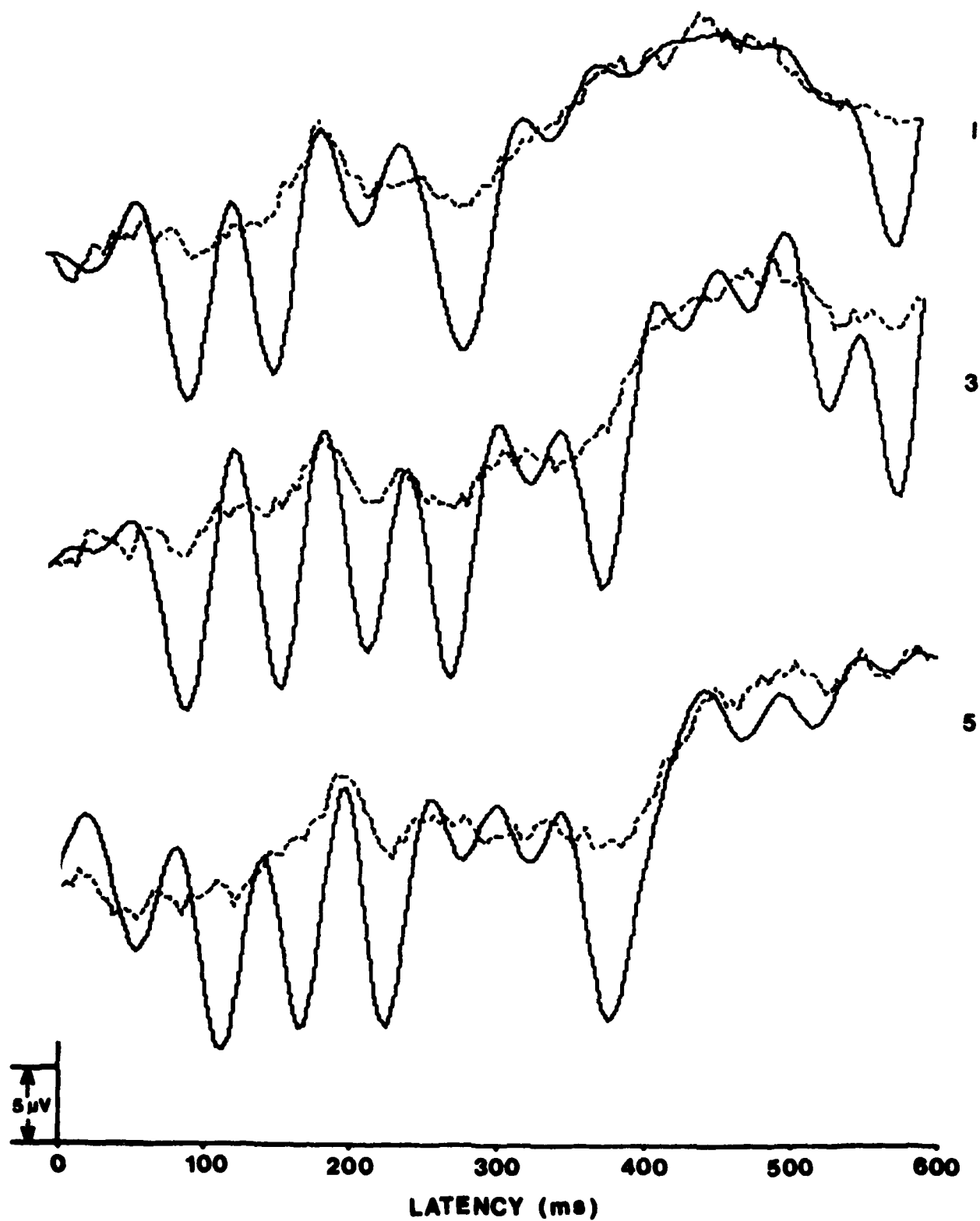


Figure 26. Continuous Latency Corrected Average (solid) and conventional average (broken) for Subject 2, non-target set. The number of targets in the set is indicated on the right.

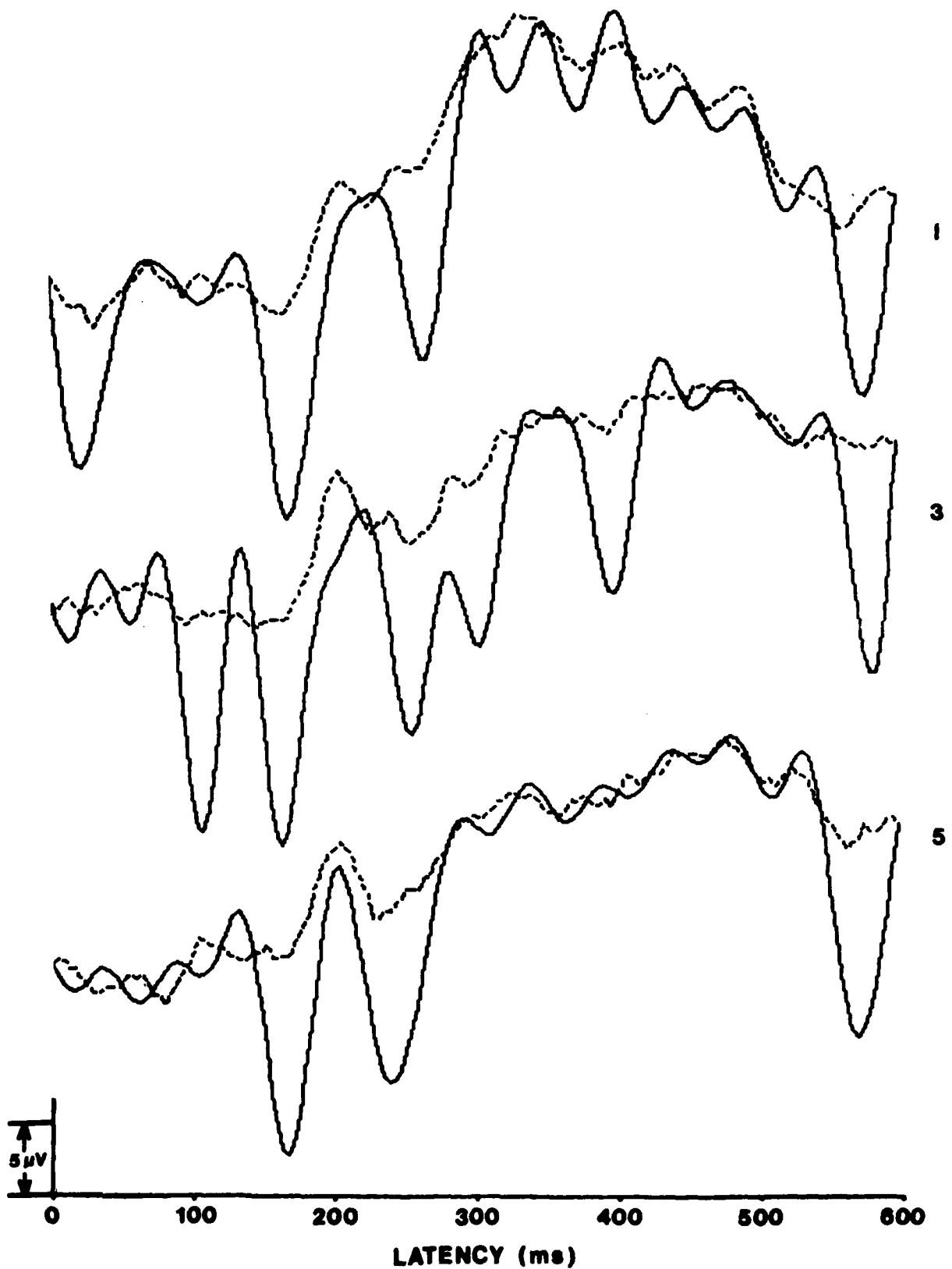


Figure 27. Continuous Latency Corrected Average (solid) and conventional average (broken) for Subject 3, target set. The number of targets in the set is indicated on the right.

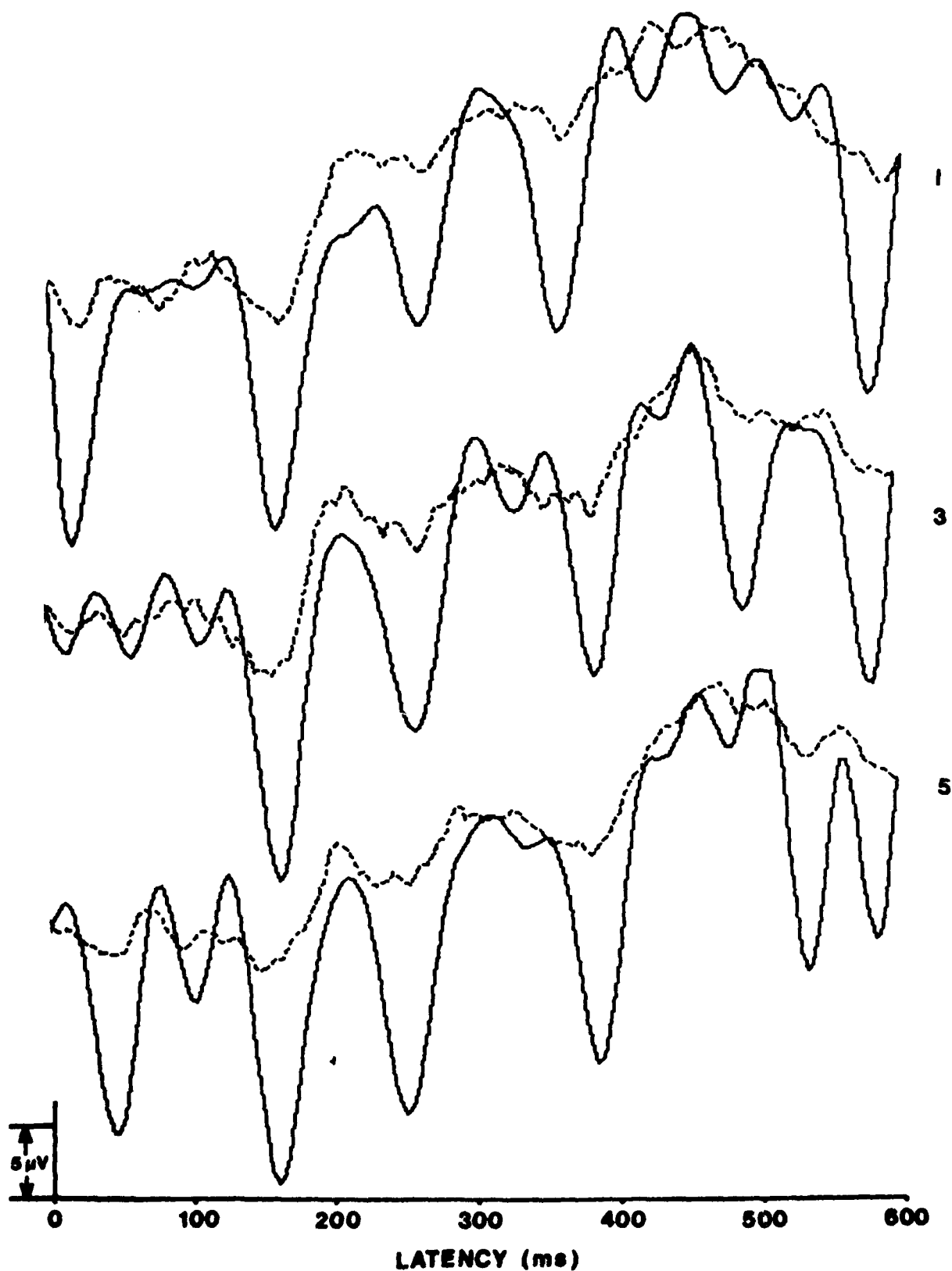


Figure 28. Continuous Latency Corrected Average (solid) and conventional average (broken) for Subject 3, non-target set. The number of targets in the set is indicated on the right.

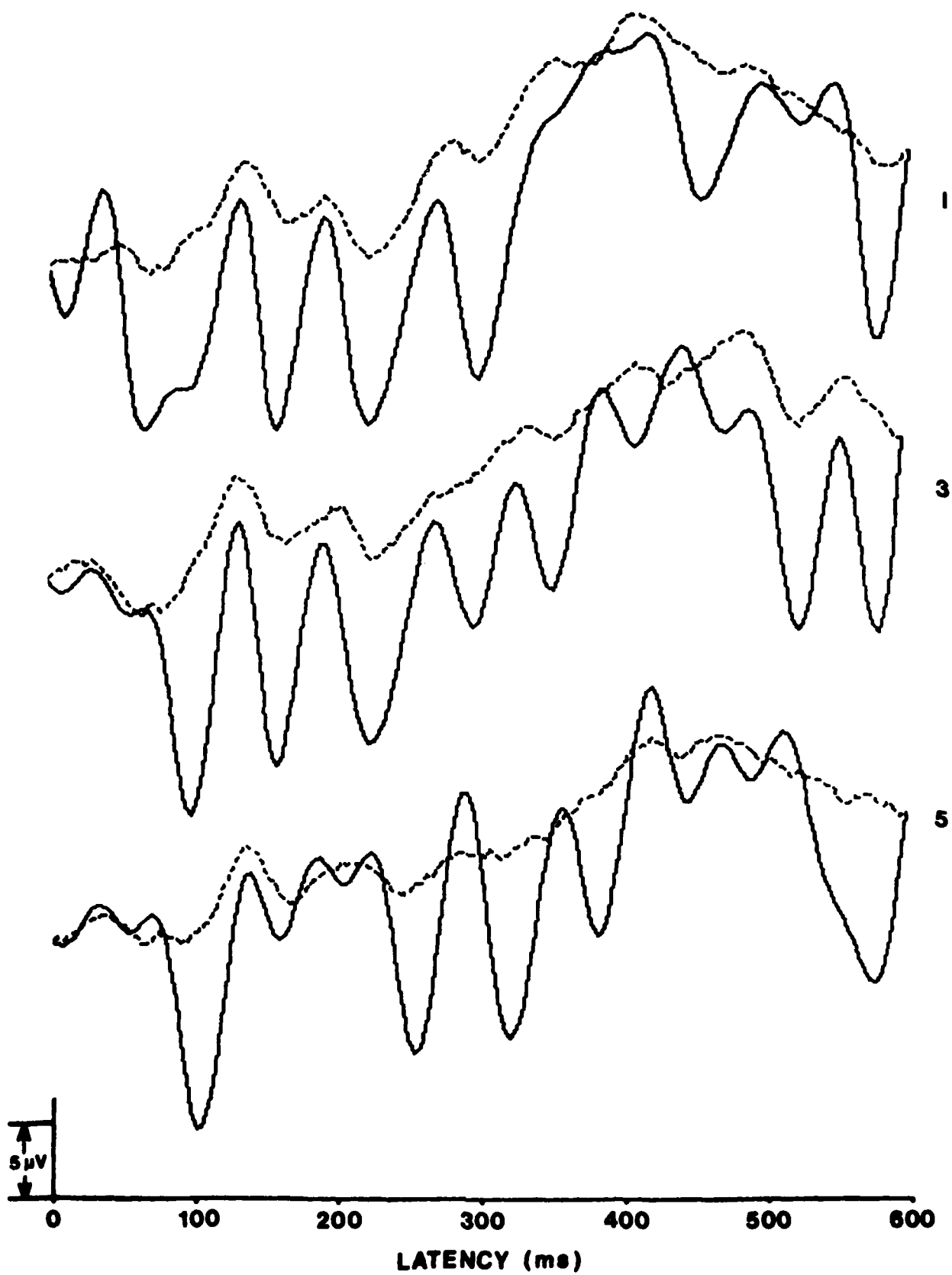


Figure 29. Continuous Latency Corrected Average (solid) and conventional average (broken) for Subject 4, target set. The number of targets in the set is indicated on the right.



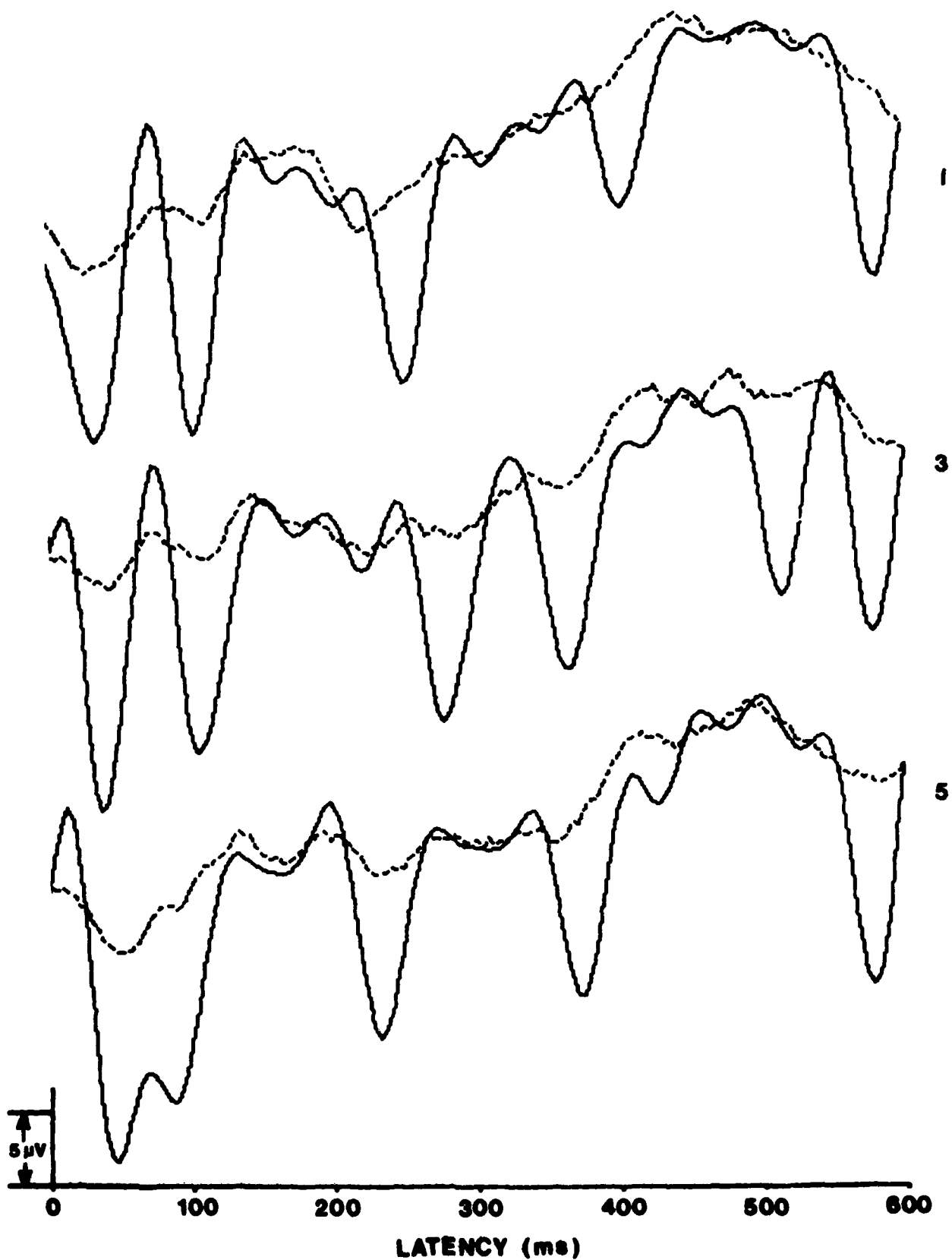


Figure 30. Continuous Latency Corrected Average (solid) and conventional average (broken) for Subject 4, non-target set. The number of targets in the set is indicated on the right.

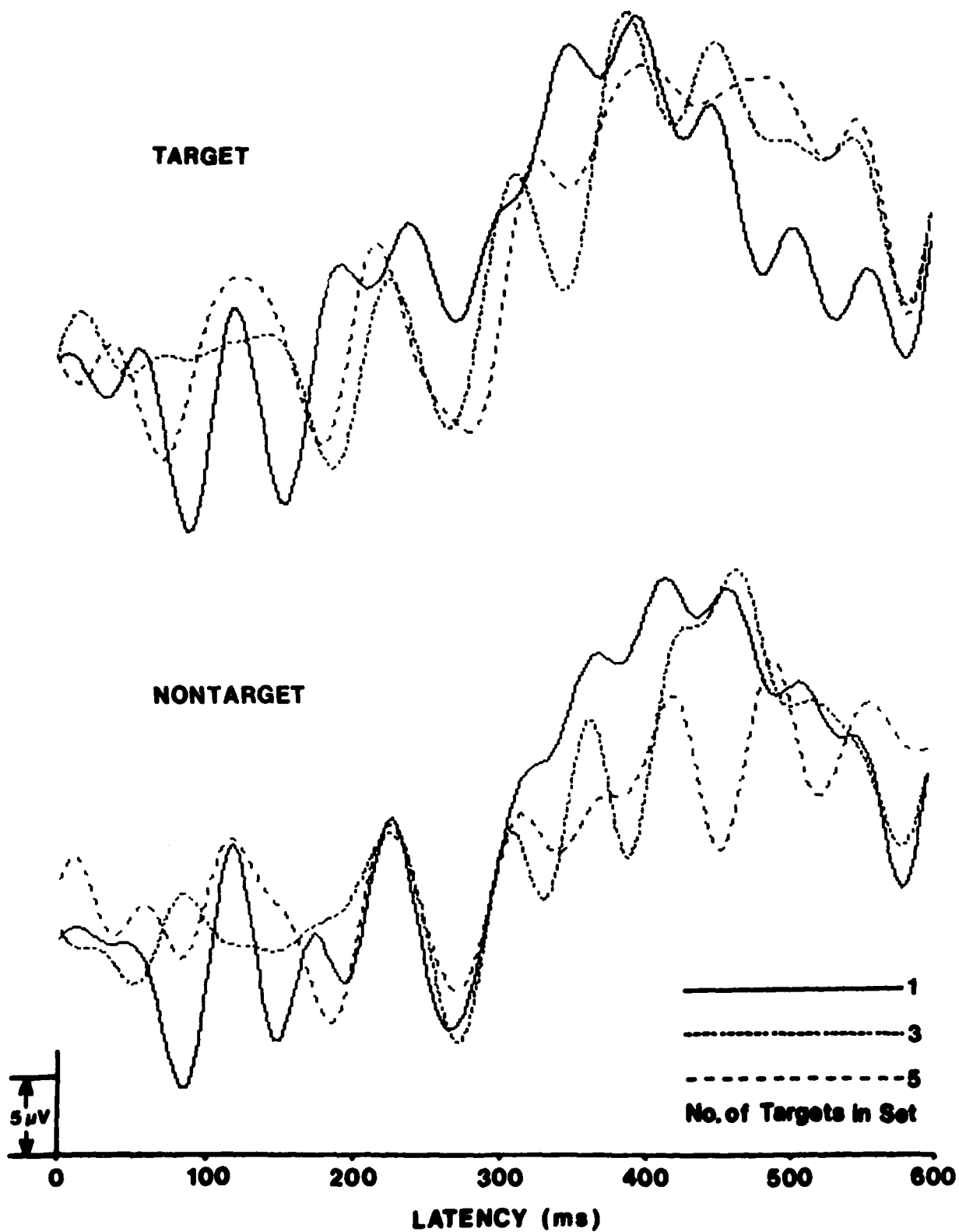


Figure 31. Continuous Latency Corrected Average for Sternberg paradigm, Subject 1, target and non-target across the three set sizes.

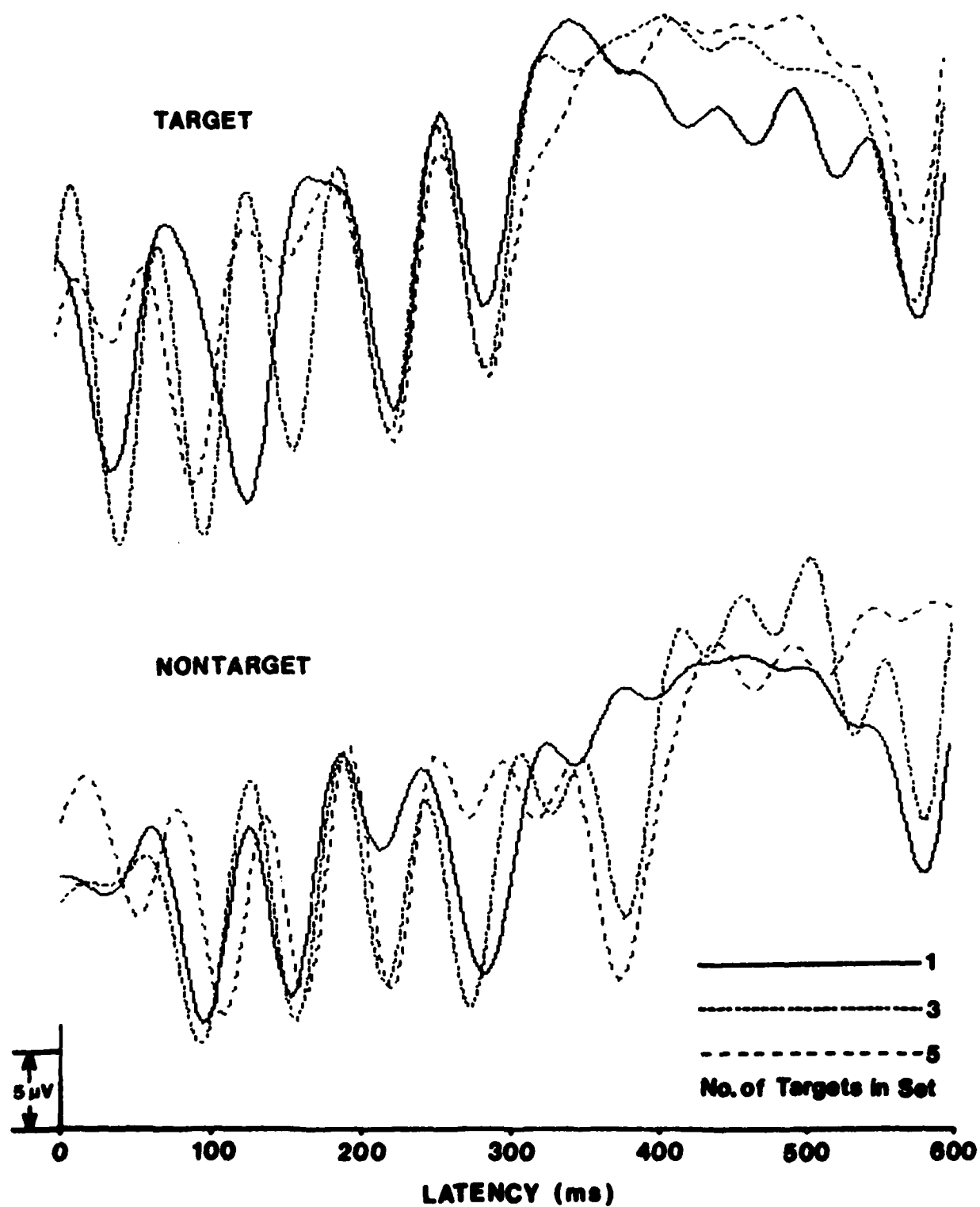


Figure 32. Continuous Latency Corrected Average for Sternberg paradigm, Subject 2, target and non-target across the three set sizes.

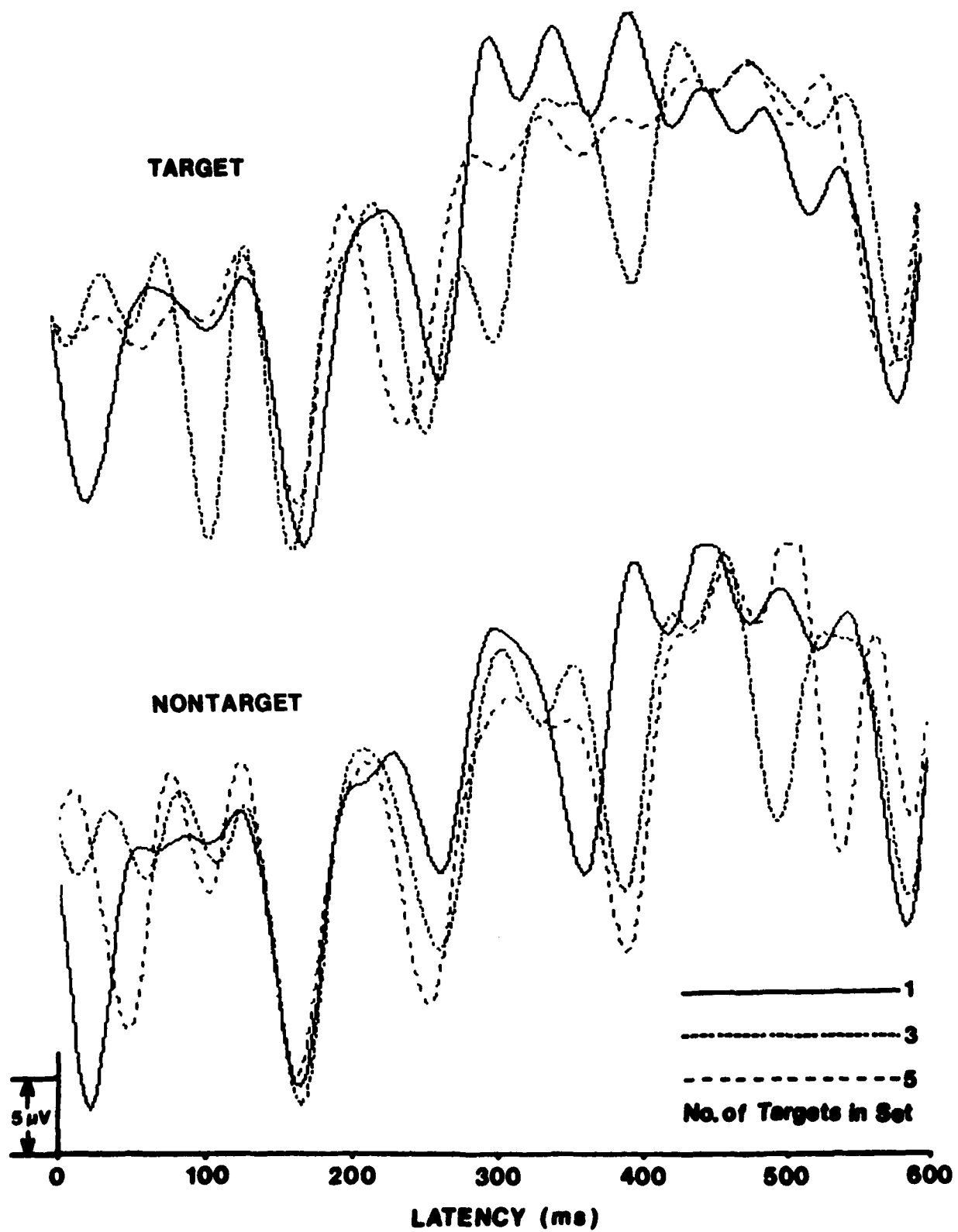


Figure 33. Continuous Latency Corrected Average for Sternberg paradigm, Subject 3, target and non-target across the three set sizes.

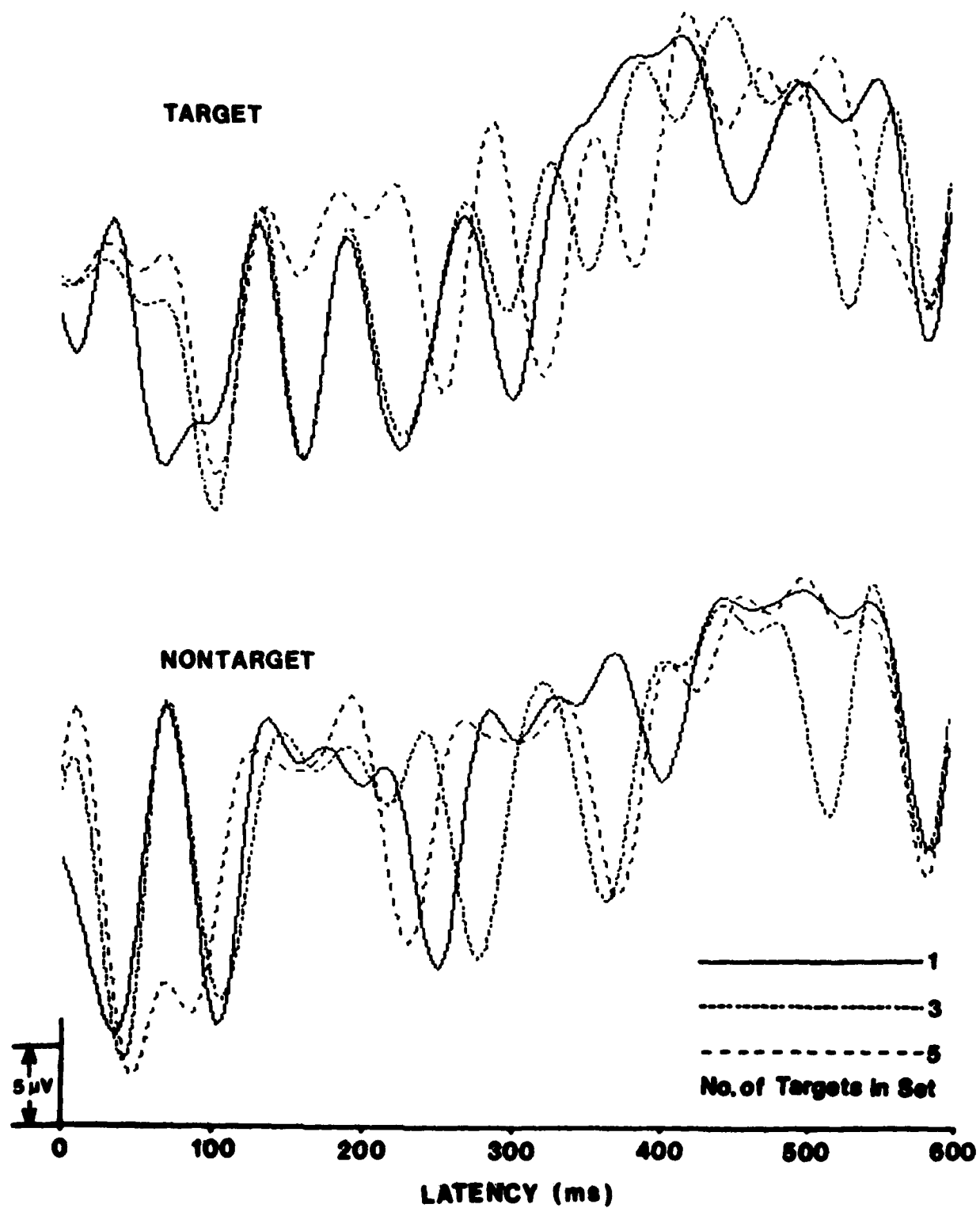


Figure 34. Continuous Latency Corrected Average for Sternberg paradigm, Subject 4, target and non-target across the three set sizes.

### Reaction Time and the CLCA

From the LCA statistics, two peaks were chosen as P3a and P3b for each subject and for each set of targets. The mean reaction time for each of the trials for each subject was computed and an overall mean reaction time calculated. In order to account for mean differences across subjects, the average component latencies and reaction times across the target sets were computed. The resulting mean values for each subject were subtracted from that subjects' latencies and reaction times. Correlation coefficients were computed using 12 ordered pairs for P3a and RT (reaction time), and 11 ordered pairs for P3b and RT. The estimate used was:

$$\hat{r} = \frac{E[XY] - \bar{X} \bar{Y}}{\sigma_X \sigma_Y}$$

where each order pair is (X,Y). The estimates of the standard deviation for X and Y were computed from the values of the data. The resulting estimates of the correlation coefficients were as follows:

$$\begin{array}{ll} \text{(P3a,RT)} & r = 0.287 \quad p < 0.19 \\ \text{(P3b,RT)} & r = 0.753 \quad p < 0.003 \end{array}$$

These results indicate a high degree of correlation with the P3b wave, determined from the LCA results, with the reaction time following presentation of the stimulus.

## APPENDIX

### File Specification Key for Appendix

Subject 1 ..... sp4[a][b].pz

Subject 2 ..... sp5[a][b].pz

Subject 3 ..... sp7[a][b].pz

Subject 4 ..... sp8[a][b].pz

where [a] = t for target,  
          = n for nontarget,  
and [b] = the number of digitis in  
          the target set -1 or 3 or 5.

# LCA RESULTS FOR sp4t1.pz

## positive peaks

pk. #	range	mean	st. d	pct.	max.	min.	amp. st. d
1	29- 35	123.55	8.10	44.00	-1.91	-9.32	10.63
2	85- 91	347.76	8.36	33.00	16.32	8.10	20.25
3	95-106	397.90	13.38	61.00	18.11	11.57	22.38

## negative peaks

pk. #	range	mean	st. d	pct.	max.	min.	amp. st. d
1	21- 27	91.78	7.54	37.00	-7.99	-17.91	16.08
2	37- 43	155.90	6.98	42.00	-5.35	-15.83	17.00
3	69- 72	277.45	4.71	22.00	3.83	-8.45	15.73
4	78- 81	314.10	5.31	21.00	8.22	-2.26	9.28
5	121-124	486.60	4.36	20.00	6.79	-2.44	8.47
6	132-137	532.73	5.87	33.00	3.57	-5.01	9.33
7	142-147	578.61	5.16	72.00	.88	-5.03	11.68

```

Input data file
Lowpass filter file
Number of records
Number of samples per channel
Samples to process
Starting at sample
Number of filter coefficients
Points per histogram window
Sampling interval (ms)
Threshold for sign test
Output identifier

: sp4t1.pzcs
: lpf25.imp
: 100
: 150
: 150
: 1
: 33
: 4
: 4.0000
: .9000
: sp4t1.pz

```



# LCA RESULTS FOR sp4t3.pz

## positive peaks

pk. #	range	mean	st. d	pct.	max.	min.	amp. st. d
1	5- 8	21.03	4.79	35.00	-82	-8.99	10.48
2	54- 63	228.94	10.43	72.00	88	-7.11	9.83
3	77- 82	314.59	5.90	34.00	8.30	1.19	16.05
4	95-105	393.47	11.82	57.00	18.05	10.75	23.87
5	114-117	457.50	4.38	24.00	17.09	8.68	20.24

## negative peaks

pk. #	range	mean	st. d	pct.	max.	min.	amp. st. d
1	44- 53	190.33	11.08	67.00	-4.74	-12.94	14.45
2	63- 74	270.22	12.63	74.00	-1.81	-11.49	14.75
3	85- 91	347.67	7.49	36.00	5.28	-2.18	12.30
4	143-147	579.16	5.44	57.00	2.72	-1.99	12.27

## Input data file

Lowpass filter file  
 Number of records  
 Number of samples per channel  
 Samples to process  
 Starting at sample  
 Number of filter coefficients  
 Points per histogram window  
 Sampling interval (ms)  
 Threshold for sign test  
 Output identifier

sp4t3.pzcs  
 lpf25.imp  
 100  
 150  
 150  
 1  
 33  
 4  
 4.0000  
 9000  
 sp4t3.pz

# LCA RESULTS FOR sp4t5.pz

## positive peaks

pk. #	range	mean	st.d	pct.	max.	min.	amp. st. d
1	30- 36	128.10	7.35	43.16	1.35	-5.40	11.24
2	52- 61	221.65	11.97	71.58	2.86	-5.38	12.71
3	79- 82	319.00	4.75	25.26	8.04	-4.44	18.77
4	98-105	401.73	7.89	53.68	15.66	9.00	20.87
5	119-125	483.90	7.97	42.11	15.03	8.07	20.03
6	138-144	559.61	8.85	32.63	9.82	1.37	16.47

## negative peaks

pk. #	range	mean	st.d	pct.	max.	min.	amp. st. d
1	18- 21	73.57	4.53	29.47	-6.43	-15.59	17.00
2	43- 49	180.68	8.09	43.16	-3.22	-12.39	14.11
3	64- 69	262.46	7.03	41.05	-3.58	-11.36	12.97
4	71- 76	290.81	6.39	38.95	-1.85	-10.31	14.65
5	143-147	580.54	4.62	54.74	3.49	-3.38	12.07

## Input data file

Lowpass filter file

Number of records

Number of samples per channel

Samples to process

Starting at sample

Number of filter coefficients

Points per histogram window

Sampling interval (ms)

Threshold for sign test

Output identifier

sp4t5.pzcs

lpf25.imp

95

150

150

1

33

4

4 0000

9000

sp4t5.pz

# LCA RESULTS FOR sp4n1.pz

## positive peaks

pk. #	range	mean	st. d	pct.	max.	min.	amp. st. d
1	6- 11	30.35	5.67	34.00	-4.31	-12.06	9.91
2	31- 34	125.83	5.00	24.00	- .35	-8.66	8.11
3	54- 64	231.05	11.38	63.00	2.90	-5.85	11.16
4	92- 95	370.40	4.19	20.00	16.26	5.39	22.83
5	101-110	418.55	10.51	58.00	20.16	12.86	25.63
6	112-116	451.27	4.88	22.00	20.50	13.21	25.19

## negative peaks

pk. #	range	mean	st. d	pct.	max.	min.	amp. st. d
1	21- 26	89.08	5.25	26.00	-5.57	-18.45	17.78
2	39- 42	157.64	4.73	22.00	-6.61	-16.77	15.19
3	50- 53	204.00	4.73	21.00	-2.94	-14.72	14.42
4	65- 76	279.12	13.40	73.00	-2.24	-12.06	12.61
5	143-147	579.47	4.51	60.00	1.98	-1.73	10.23

```

Input data file
Lowpass filter file
Number of records
Number of samples per channel
Samples to process
Starting at sample
Number of filter coefficients
Points per histogram window
Sampling interval (ms)
Threshold for sign test
Output identifier

: sp4n1.pzcs
: lpf25.imp
: 100
: 150
: 150
: 1
: 33
: 4
: 4.0000
: .9000
: sp4n1.pz

```

# LCA RESULTS FOR sp4n3.pz

## positive peaks

pk. #	range	mean	st. d	pct.	max.	min.	amp. st. d
1	1- 6	13.29	4.55	31.00	-1.83	-12.20	11.05
2	23- 26	92.96	4.36	25.00	-1.64	-9.33	12.16
3	55- 62	230.67	8.99	54.00	2.26	-7.78	11.67
4	93- 97	376.62	5.73	26.00	11.81	5.44	17.49
5	103-106	414.61	4.61	23.00	14.91	8.54	18.21
6	113-121	464.73	9.52	55.00	20.33	13.02	22.73

## negative peaks

pk. #	range	mean	st. d	pct.	max.	min.	amp. st. d
1	63- 77	280.39	15.46	82.00	-3.60	-13.37	13.96
2	97-102	393.92	6.44	25.00	8.72	-2.89	8.74
3	142-147	576.84	7.50	62.00	4.88	.52	9.49

Input data file  
 Lowpass filter file  
 Number of records  
 Number of samples per channel  
 Samples to process  
 Starting at sample  
 Number of filter coefficients  
 Points per histogram window  
 Sampling interval (ms)  
 Threshold for sign test  
 Output identifier

sp4n3.pzcs  
 lpf25.imp  
 100  
 150  
 150  
 1  
 33  
 4  
 4.0000  
 9000  
 sp4n3.pz

# LCA RESULTS FOR sp4n5.pz

## positive peaks

pk. #	range	mean	st.d	pct.	max.	min.	amp. st.d
1	1- 8	15.68	5.87	50.00	.54	-7.38	11.20
2	30- 34	124.97	4.25	33.00	2.29	-4.68	9.94
3	54- 64	231.36	12.06	81.00	2.87	-4.12	10.73
4	78- 82	315.87	4.98	30.00	3.35	-2.19	11.31
5	104-110	422.48	8.04	50.00	11.79	4.73	16.08
6	122-128	496.80	7.96	40.00	14.10	6.38	18.79

## negative peaks

pk. #	range	mean	st.d	pct.	max.	min.	amp. st.d
1	45- 53	191.94	9.91	66.00	-4.00	-12.25	13.58
2	67- 74	278.79	8.63	56.00	-2.78	-10.49	13.59
3	112-118	454.63	7.36	41.00	8.09	.55	10.60
4	129-132	518.21	4.48	29.00	9.95	.75	10.44
5	147-147	584.00	.00	15.00	3.69	-2.30	11.03

```

Input data file
Lowpass filter file
Number of records
Number of samples per channel
Samples to process
Starting at sample
Number of filter coefficients
Points per histogram window
Sampling interval (ms)
Threshold for sign test
Output identifier

: sp4n5.pzcs
: lpf25.imp
: 100
: 150
: 150
: 1
: 33
: 4
: 4.0000
: 9000
: sp4n5.pz

```

# LCA RESULTS FOR sp6t1.pz

## positive peaks

pk. #	range	mean	st. d	pct.	max.	min.	amp. st. d
1	19- 24	81.95	6.64	41.84	2.00	-11.62	15.14
2	46- 53	195.55	7.83	54.08	5.98	-6.68	15.33
3	62- 65	250.55	4.54	22.45	4.48	-6.54	11.58
4	88- 92	355.75	5.07	32.65	16.09	3.01	23.53
5	95-101	388.57	8.17	42.86	13.51	3.26	24.64
6	124-128	500.12	6.36	33.67	10.62	1.26	21.05
7	138-144	559.44	6.68	43.88	7.82	-2.64	19.26

## negative peaks

pk. #	range	mean	st. d	pct.	max.	min.	amp. st. d
1	8- 13	37.74	5.72	39.80	-1.70	-17.99	18.71
2	30- 38	130.55	8.86	59.18	-2.91	-18.77	19.64
3	54- 61	226.69	8.72	59.18	1.33	-10.69	13.31
4	73- 77	296.00	5.76	28.57	8.24	-7.55	11.60
5	143-148	582.76	5.88	72.45	1.68	-5.54	11.59

```

Input data file
Lowpass filter file
Number of records
Number of samples per channel
Samples to process
Starting at sample
Number of filter coefficients
Points per histogram window
Sampling interval (ms)
Threshold for sign test
Output identifier

```

```

: sp6t1.pzcs
: lpf25.imp
: 98
: 151
: 151
: 1
: 33
: 4
: 4.0000
: .9000
: sp6t1.pz

```

# LCA RESULTS FOR sp6t3.pz

## positive peaks

pk. #	range	mean	st. d	pct.	max.	min.	amp. st. d
1	4- 7	17.10	4.77	29.00	1.10	-13.06	17.09
2	16- 22	70.84	7.22	45.00	1.36	-11.65	15.97
3	45- 53	192.56	8.67	64.00	5.87	-7.49	18.22
4	81- 85	329.03	5.46	31.00	13.14	.74	22.01
5	101-104	405.71	4.54	28.00	18.32	5.65	25.76
6	127-132	514.05	6.61	43.00	12.92	3.45	23.58

## negative peaks

pk. #	range	mean	st. d	pct.	max.	min.	amp. st. d
1	10- 15	45.37	5.90	38.00	-4.13	-21.04	23.45
2	22- 29	98.27	9.17	51.00	-4.21	-21.06	15.55
3	39- 45	163.04	6.70	46.00	- 12	-14.69	18.08
4	55- 59	225.25	5.02	32.00	- 45	-13.57	14.90
5	72- 77	294.18	5.66	33.00	4.37	-10.03	14.39
6	142-148	580.30	7.37	66.00	1.85	-4.38	14.51

## Input data file

Lowpass filter file  
Number of records  
Number of samples per channel  
Samples to process  
Starting at sample  
Number of filter coefficients  
Points per histogram window  
Sampling interval (ms)  
Threshold for sign test  
Output identifier

sp6t3.pzcs  
lpf25.imp  
100  
151  
151  
1  
33  
4  
4.0000  
9000  
sp6t3.pz

# LCA RESULTS FOR sp6t5.pz

## positive peaks

pk. #	range	mean	st. d	pct.	max.	min.	amp. st. d
1	1- 7	15.20	5.16	45.00	.42	-14.69	13.82
2	45- 53	190.55	8.70	58.00	5.45	-6.70	14.94
3	80- 85	326.11	6.73	36.00	7.41	.09	17.09
4	97-100	388.87	4.51	23.00	12.32	4.41	21.91
5	126-129	506.26	4.48	23.00	17.32	5.94	25.48

## negative peaks

pk. #	range	mean	st. d	pct.	max.	min.	amp. st. d
1	23- 26	93.10	4.26	29.00	-4.59	-20.00	20.42
2	55- 61	228.09	8.16	43.00	-2.01	-13.64	12.36
3	70- 79	294.65	12.44	65.00	2.56	-8.53	11.66
4	143-148	580.73	6.61	60.00	5.38	.76	13.88

```

Input data file
Lowpass filter file
Number of records
Number of samples per channel
Samples to process
Starting at sample
Number of filter coefficients
Points per histogram window
Sampling interval (ms)
Threshold for sign test
Output identifier

```

```

: sp6t5.pzcs
: 1pf25.imp
: 100
: 151
: 151
: 1
: 33
: 4
: 4.0000
: .9000
: sp6t5.pz

```



# LCA RESULTS FOR sp6n1.pz

## positive peaks

pk. #	range	mean	st. d	pct.	max.	min.	amp. st. d
1	46- 52	191.56	6.05	55.00	6.67	-4.99	16.55
2	63- 66	253.39	4.45	23.00	4.95	-3.88	14.54
3	110-115	445.94	7.22	31.00	15.14	4.07	21.92
4	124-129	503.09	6.22	35.00	13.57	4.84	23.56

## negative peaks

pk. #	range	mean	st. d	pct.	max.	min.	amp. st. d
1	23- 28	98.06	7.15	33.00	-1.91	-13.40	14.11
2	38- 43	156.92	6.52	39.00	.20	-12.71	13.82
3	69- 77	288.00	9.57	59.00	.75	-9.53	10.85
4	143-148	580.95	6.49	59.00	3.71	-2.32	14.10

Input data file  
 Lowpass filter file  
 Number of records  
 Number of samples per channel  
 Samples to process  
 Starting at sample  
 Number of filter coefficients  
 Points per histogram window  
 Sampling interval (ms)  
 Threshold for sign test  
 Output identifier

sp6n1.pzs
lpf25.imp
100
151
151
1
33
4
4.0000
.9000
sp6n1.pz

# LCA RESULTS FOR sp6n3.pz

## positive peaks

pk. #	range	mean	st. d	pct.	max.	min.	amp. st. d
1	45- 53	191.56	9.90	64.00	5.62	-6.28	15.84
2	61- 66	250.29	6.46	35.00	2.39	-6.59	13.33
3	100-103	402.20	3.55	20.00	11.62	5.17	19.79
4	116-121	470.32	6.87	38.00	17.43	7.65	24.29
5	125-131	506.92	7.64	37.00	20.79	11.22	28.32

## negative peaks

pk. #	range	mean	st. d	pct.	max.	min.	amp. st. d
1	22- 27	95.12	6.03	41.00	- .08	-15.18	14.10
2	39- 44	161.37	6.99	35.00	-1.67	-13.32	11.67
3	54- 58	221.06	5.24	34.00	.57	-10.78	12.01
4	67- 73	277.24	7.71	45.00	- .13	-11.90	12.16
5	94-100	383.28	6.80	39.00	5.52	-4.99	9.63
6	134-137	539.00	4.70	28.00	14.75	5.03	14.46
7	144-148	584.09	4.45	47.00	6.84	.45	11.43

Input data file  
 Lowpass filter file  
 Number of records  
 Number of samples per channel  
 Samples to process  
 Starting at sample  
 Number of filter coefficients  
 Points per histogram window  
 Sampling interval (ms)  
 Threshold for sign test  
 Output identifier

sp6n3.pzcs  
 lpf25.imp  
 100  
 151  
 151  
 1  
 33  
 4  
 4.0000  
 .9000  
 sp6n3.pz

# LCA RESULTS FOR sp6n5.pz

## positive peaks

pk. #	range	mean	st. d	pct.	max.	min.	amp. st. d
1	1- 7	14.75	5.40	51.00	7.02	-9.37	12.05
2	46- 54	195.75	8.36	65.00	6.75	-3.57	14.88
3	61- 64	246.46	4.24	26.00	3.07	-6.74	10.90
4	83- 87	334.21	5.30	29.00	4.42	-4.82	15.69
5	120-129	494.85	11.19	59.00	15.65	6.76	24.43

## negative peaks

pk. #	range	mean	st. d	pct.	max.	min.	amp. st. d
1	28- 31	115.29	4.50	28.00	-1.65	-14.28	12.28
2	40- 46	166.51	8.05	43.00	1.47	-10.93	12.62
3	53- 59	222.05	7.63	43.00	1.77	-10.66	10.42
4	92-101	380.57	10.69	56.00	.85	-10.25	11.38

```

Input data file
Lowpass filter file
Number of records
Number of samples per channel
Samples to process
Starting at sample
Number of filter coefficients
Points per histogram window
Sampling interval (ms)
Threshold for sign test
Output identifier

: sp6n5.pzcs
: lpf25.imp
: 100
: 151
: 151
: 1
: 33
: 4
: 4.0000
: .9000
: sp6n5.pz

```

# LCA RESULTS FOR sp7t1.pz

## positive peaks

pk. #	range	mean	st.d	pct.	max.	min.	amp. st. d
1	1- 4	9.65	2.03	17.00	.00	.00	15.04
2	49- 55	204.97	6.76	37.00	5.11	-6.71	16.61
3	77- 80	309.09	4.13	22.00	14.45	3.14	25.18
4	86- 91	350.32	5.85	38.00	19.08	4.99	27.04
5	109-112	437.85	4.27	26.00	13.00	- .97	22.62
6	122-128	495.04	7.46	46.00	14.35	- .94	24.07

## negative peaks

pk. #	range	mean	st.d	pct.	max.	min.	amp. st. d
1	6- 9	26.61	5.20	23.00	-3.22	-20.69	14.94
2	41- 49	175.64	8.44	55.00	-2.00	-17.12	14.12
3	65- 70	265.88	6.77	34.00	4.88	-7.68	8.20
4	143-148	582.50	5.67	72.00	2.24	-7.48	11.04

```

Input data file
Lowpass filter file
Number of records
Number of samples per channel
Samples to process
Starting at sample
Number of filter coefficients
Points per histogram window
Sampling interval (ms)
Threshold for sign test
Output identifier

: sp7t1.pzcs
: 1pf25.imp
: 100
: 151
: 151
: 1
: 33
: 4
: 4.0000
: .9000
: sp7t1.pz

```

# LCA RESULTS FOR sp7t3.pz

## positive peaks

pk. #	range	mean	st. d	pct.	max.	min.	amp. st. d
1	50- 56	207.70	6.16	56.25	5.86	-4.66	16.72
2	70- 73	282.09	4.95	23.96	7.08	-2.29	20.06
3	88- 91	353.04	5.03	28.13	14.31	3.40	25.11

## negative peaks

pk. #	range	mean	st. d	pct.	max.	min.	amp. st. d
1	26- 29	105.00	4.61	25.00	-3.71	-21.07	20.77
2	39- 47	168.32	9.45	64.58	-3.34	-16.03	11.58
3	63- 69	259.81	7.56	44.79	.95	-10.43	10.84
4	75- 79	304.00	5.37	32.29	4.40	-8.30	11.29
5	99-102	397.38	4.31	30.21	8.23	-4.09	8.99
6	144-148	582.31	5.69	46.88	5.19	-5.38	10.64

```

Input data file
Lowpass filter file
Number of records
Number of samples per channel
Samples to process
Starting at sample
Number of filter coefficients
Points per histogram window
Sampling interval (ms)
Threshold for sign test
Output identifier
: sp7t3.pzcs
: lpf25.imp
: 96
: 151
: 151
: 1
: 33
: 4
: 4.0000
: .9000
: sp7t3.pz

```

# LCA RESULTS FOR sp7t5.pz

## positive peaks

pk. #	range	mean	st. d	pct.	max.	min.	amp. st. d
1	47- 56	202.87	10.53	67.00	7.21	-4.73	17.98
2	72- 77	293.21	6.33	43.00	11.04	.82	21.35
3	135-138	540.43	4.12	28.00	14.17	-2.52	26.92

## negative peaks

pk. #	range	mean	st. d	pct.	max.	min.	amp. st. d
1	41- 46	170.90	6.27	40.00	-2.17	-15.74	14.00
2	57- 67	245.39	12.69	75.00	1.51	-9.90	12.32
3	139-148	574.00	12.30	84.00	6.48	-6.12	11.49

```

Input data file
Lowpass filter file
Number of records
Number of samples per channel
Samples to process
Starting at sample
Number of filter coefficients
Points per histogram window
Sampling interval (ms)
Threshold for sign test
Output identifier
: sp7t5.pzcs
: lpf25.imp
: 100
: 151
: 151
: 1
: 33
: 4
: 4.0000
: .9000
: sp7t5.pz

```

LCA RESULTS FOR sp7n1.pz

positive peaks

pk. #	range	mean	st. d	pct.	max.	min.	amp. st. d
1	32- 37	132.73	6.28	33.00	1.44	-9.51	15.09
2	50- 57	209.96	8.59	51.00	6.54	-4.89	17.38
3	84- 88	339.26	9.59	27.00	10.83	1.73	20.42
4	104-107	419.45	4.10	29.00	16.52	3.99	27.37
5	120-123	481.38	4.31	29.00	16.43	5.02	28.72
6	139-143	560.00	4.78	29.00	13.15	-1.50	24.12

negative peaks

pk. #	range	mean	st. d	pct.	max.	min.	amp. st. d
1	4- 10	22.34	8.61	58.00	-5.50	-19.05	13.75
2	38- 48	166.14	10.38	71.00	-3.26	-16.67	12.99
3	65- 68	260.83	4.25	24.00	4.47	-8.99	9.68
4	88- 94	360.47	6.72	43.00	6.67	-3.98	10.81
5	143-148	581.91	5.84	67.00	2.45	-7.19	13.36

Input data file

Lowpass filter file  
Number of records  
Number of samples per channel  
Samples to process  
Starting at sample  
Number of filter coefficients  
Points per histogram window  
Sampling interval (ms)  
Threshold for sign test  
Output identifier

sp7n1.pzcs  
lpf25.imp  
100  
151  
151  
1  
33  
4  
4.0000  
.9000  
sp7n1.pz

# LCA RESULTS FOR sp7n3.pz

## positive peaks

pk. #	range	mean	st. d	pct.	max.	min.	amp. st. d
1	48-56	205.57	9.14	63.01	7.06	-2.66	18.25
2	71-75	288.15	5.82	35.62	10.51	.50	21.84
3	113-120	460.20	8.58	56.16	20.47	7.76	29.96
4	136-141	548.97	6.47	39.73	13.57	-2.15	24.18

## negative peaks

pk. #	range	mean	st. d	pct.	max.	min.	amp. st. d
1	39-47	167.57	9.36	63.01	-4.85	-17.77	16.44
2	62-71	262.27	10.86	60.27	-8.82	-8.60	11.64
3	96-101	390.43	6.38	38.36	8.21	-4.99	10.49
4	123-127	495.33	4.82	32.88	11.13	-1.99	12.67
5	145-148	584.00	4.70	41.10	5.56	-7.44	9.81

```

Input data file
Lowpass filter file
Number of records
Number of samples per channel
Samples to process
Starting at sample
Number of filter coefficients
Points per histogram window
Sampling interval (ms)
Threshold for sign test
Output identifier
: sp7n3.pzcs
: lpf25.imp
: 73
: 151
: 151
: 1
: 33
: 4
: 4.0000
: .9000
: sp7n3.pz

```



LCA RESULTS FOR sp7n5.pz

positive peaks

pk. #	range	mean	st.d	pct.	max.	min.	amp. st. d
1	1- 6	13.08	4.77	37.00	4.67	-4.78	15.59
2	16- 21	69.62	6.70	37.00	3.86	-9.61	17.73
3	50- 57	208.15	8.82	54.00	6.15	-3.91	18.31
4	69- 75	284.84	8.53	43.00	7.25	-1.39	19.81
5	85- 88	342.56	4.45	25.00	8.02	- .12	19.22
6	107-111	432.13	4.98	30.00	16.58	4.29	26.57
7	116-121	470.45	6.52	49.00	18.99	7.98	29.72
8	140-145	564.64	6.58	50.00	16.58	2.64	26.77

negative peaks

pk. #	range	mean	st.d	pct.	max.	min.	amp. st. d
1	11- 14	45.55	5.03	31.00	-3.09	-18.56	15.98
2	38- 47	164.95	11.24	63.00	-2.75	-16.50	14.30
3	62- 68	257.58	8.05	43.00	- .53	-12.77	14.48
4	94-103	390.18	10.56	57.00	3.67	-7.38	11.97
5	134-139	540.34	7.17	47.00	13.47	-2.32	14.05
6	145-148	584.11	4.73	36.00	9.69	-3.65	12.05

```

Input data file
Lowpass filter file
Number of records
Number of samples per channel
Samples to process
Starting at sample
Number of filter coefficients
Points per histogram window
Sampling interval (ms)
Threshold for sign test
Output identifier

```

sp7n5.pzcs  
 lpf25.imp  
 100  
 151  
 151  
 1  
 33  
 4  
 4.0000  
 .9000  
 sp7n5.pz

# LCA RESULTS FOR sp8t1.pz

## positive peaks

pk. #	range	mean	st. d	pct.	max.	min.	amp. st. d
1	31-38	133.25	7.18	52.04	3.74	-7.11	16.11
2	46-52	193.19	7.27	47.96	2.75	-7.23	14.05
3	66-72	273.00	8.08	36.73	4.23	-3.89	14.47
4	82-89	339.92	8.40	53.06	10.87	3.45	21.12
5	100-106	407.91	7.74	44.90	17.48	7.43	28.39
6	121-125	487.30	4.92	23.47	11.95	4.29	19.94
7	141-144	566.36	4.56	22.45	11.81	1.99	22.27

## negative peaks

pk. #	range	mean	st. d	pct.	max.	min.	amp. st. d
1	18-21	74.33	4.07	24.49	-2.63	-19.17	17.96
2	26-29	106.14	5.05	28.57	-1.04	-12.82	9.55
3	40-43	162.72	4.72	25.51	-3.43	-15.34	13.02
4	53-64	231.73	11.89	75.51	-2.45	-11.53	10.17
5	73-76	292.80	4.23	20.41	1.74	-6.76	8.05
6	78-82	315.26	5.66	27.55	1.55	-7.59	9.82
7	113-116	454.91	4.31	22.45	7.82	-3.32	14.58
8	144-148	583.75	4.33	65.31	1.54	-4.52	12.99

```

Input data file
Lowpass filter file
Number of records
Number of samples per channel
Samples to process
Starting at sample
Number of filter coefficients
Points per histogram window
Sampling interval (ms)
Threshold for sign test
Output identifier

: sp8t1.pzcs
: lpf25. imp
: 98
: 151
: 151
: 1
: 33
: 4
: 4.0000
: .9000
: sp8t1.pz

```

# LCA RESULTS FOR sp8t3.pz

## positive peaks

pk. #	range	mean	st. d.	pct.	max.	min.	amp. st. d
1	7- 11	32.26	5.74	32.29	1.68	-8.15	15.11
2	31- 39	136.13	9.21	66.67	4.36	-4.54	16.66
3	46- 52	190.09	7.34	45.83	3.58	-3.71	15.89
4	64- 69	262.59	6.41	38.54	3.23	-4.58	14.90
5	79- 86	326.43	9.24	58.33	8.21	.96	20.15
6	101-105	408.28	5.34	30.21	11.61	3.51	21.79
7	119-126	486.84	8.32	57.29	14.33	6.33	25.12
8	137-144	557.19	9.04	59.38	11.84	3.96	24.57

## negative peaks

pk. #	range	mean	st. d.	pct.	max.	min.	amp. st. d
1	23- 26	93.93	4.21	28.13	-4.25	-15.18	13.33
2	28- 31	112.48	4.52	26.04	-3.84	-13.09	10.39
3	39- 45	163.60	8.49	41.67	-2.99	-13.21	13.08
4	54- 63	231.41	10.30	70.83	-2.70	-11.35	10.00
5	75- 78	303.20	4.76	26.04	1.45	-5.63	9.18
6	89- 92	356.83	5.28	30.21	5.96	-2.17	14.37
7	129-137	529.29	9.27	64.58	6.78	-1.33	12.25
8	144-148	582.32	5.55	52.08	3.84	-1.96	10.80

```

Input data file
Lowpass filter file
Number of records
Number of samples per channel
Samples to process
Starting at sample
Number of filter coefficients
Points per histogram window
Sampling interval (ms)
Threshold for sign test
Output identifier

: sp8t3.pzcs
: lp825.imp
: 96
: 151
: 151
: 1
: 33
: 4
: 4.0000
: .9000
: sp8t3.pz

```

# LCA RESULTS FOR sp8t5.pz

## positive peaks

pk. #	range	mean	st. d	pct.	max.	min.	amp. st. d
1	8- 13	38.63	6.12	46.91	3.16	-6.02	14.01
2	31- 38	134.40	7.83	55.56	4.78	-4.41	14.97
3	53- 57	216.30	5.97	33.33	6.90	-3.78	16.34
4	85- 88	342.20	4.20	24.69	4.91	-1.93	12.63
5	101-104	405.64	4.88	27.16	15.55	6.58	24.64
6	115-118	460.73	4.56	27.16	12.61	6.31	22.74
7	134-137	538.11	4.29	23.46	12.75	5.94	20.98

## negative peaks

pk. #	range	mean	st. d	pct.	max.	min.	amp. st. d
1	25- 31	107.69	7.36	48.15	-1.72	-13.86	14.31
2	63- 67	256.29	5.44	34.57	.31	-8.43	11.56
3	80- 84	325.14	6.14	34.57	-3.99	-7.70	8.25
4	96- 99	384.84	4.91	23.46	5.76	-3.54	9.86
5	137-142	555.00	6.31	34.57	7.35	.06	11.92
6	145-148	584.33	4.62	44.44	1.93	-3.31	9.99

```

Input data file
Lowpass filter file
Number of records
Number of samples per channel
Samples to process
Starting at sample
Number of filter coefficients
Points per histogram window
Sampling interval (ms)
Threshold for sign test
Output identifier

: sp8t5.pzcs
: lp825.imp
: 81
: 151
: 151
: 1
: 33
: 4
: 4.0000
: .9000
: sp8t5.pz

```

# LCA RESULTS FOR sp8n1.pz

## positive peaks

pk. #	range	mean	st. d	pct.	max.	min.	amp. st. d
1	1- 6	12.75	4.48	32.00	2.10	-6.91	12.01
2	21- 24	85.63	5.23	27.00	3.74	-8.17	15.12
3	44- 50	184.59	7.13	41.00	6.33	-3.41	17.83
4	106-111	430.06	6.68	35.00	13.69	6.74	24.14

## negative peaks

pk. #	range	mean	st. d	pct.	max.	min.	amp. st. d
1	6- 10	27.31	4.91	29.00	-6.88	-19.60	16.25
2	25- 30	106.15	6.46	41.00	-2.11	-13.50	10.46
3	62- 67	253.33	7.32	42.00	-1.90	-10.15	8.85
4	101-104	404.67	4.36	24.00	6.00	- .83	13.71
5	144-148	583.00	4.78	48.00	2.62	-1.92	10.60

```

Input data file
Lowpass filter file
Number of records
Number of samples per channel
Samples to process
Starting at sample
Number of filter coefficients
Points per histogram window
Sampling interval (ms)
Threshold for sign test
Output identifier

: sp8n1.pzcs
: lpf25.imp
: 100
: 151
: 151
: 1
: 33
: 4
: 4.0000
: 9000
: sp8n1.pz

```

# LCA RESULTS FOR sp8n3.pz

## positive peaks

pk. #	range	mean	st. d	pct.	max.	min.	amp. st. d
1	4- 7	16.63	3.82	40.51	3.31	-5.96	13.68
2	34- 37	137.73	4.29	37.97	4.76	-4.44	15.24
3	100-106	409.23	7.90	49.37	11.92	3.62	20.17
4	116-121	469.06	6.48	43.04	14.23	7.05	24.97
5	132-137	534.75	6.85	40.51	12.34	5.12	23.59

## negative peaks

pk. #	range	mean	st. d	pct.	max.	min.	amp. st. d
1	8- 13	40.00	6.39	37.97	-4.65	-15.84	14.48
2	26- 31	108.44	6.61	45.57	-3.35	-12.90	11.38
3	68- 74	279.89	7.06	45.57	-2.32	-9.39	7.42
4	89- 96	365.30	9.14	46.84	2.65	-5.42	8.88
5	127-131	513.10	5.94	36.71	7.47	-1.40	11.81
6	144-148	582.56	5.16	45.57	2.93	-2.66	13.23

```

Input data file
Lowpass filter file
Number of records
Number of samples per channel
Samples to process
Starting at sample
Number of filter coefficients
Points per histogram window
Sampling interval (ms)
Threshold for sign test
Output identifier
: sp8n3.pzcs
: lpf25.imp
: 79
: 151
: 151
: 1
: 33
: 4
: 4.0000
: .9000
: sp8n3.pz

```

# LCA RESULTS FOR sp8n5.pz

## positive peaks

pk. #	range	mean	st. d	pct.	max.	min.	amp. st. d
1	4- 8	19.10	5.72	42.47	4.06	-3.11	14.68
2	30- 36	129.29	7.82	42.47	5.65	-5.10	17.15
3	68- 71	275.50	5.03	21.92	7.03	-.94	14.64
4	103-108	418.77	5.85	35.62	10.36	3.36	20.40

## negative peaks

pk. #	range	mean	st. d	pct.	max.	min.	amp. st. d
1	11- 17	52.48	8.76	45.21	-4.85	-18.21	18.33
2	21- 27	91.13	8.30	43.84	-3.30	-13.50	12.22
3	57- 62	232.59	6.90	36.99	-.30	-9.59	8.83
4	92- 98	374.86	8.15	47.95	3.64	-5.02	10.28
5	143-148	580.60	6.93	54.79	2.91	-3.04	9.47

## Input data file

Lowpass filter file  
Number of records  
Number of samples per channel  
Samples to process  
Starting at sample  
Number of filter coefficients  
Points per histogram window  
Sampling interval (ms)  
Threshold for sign test  
Output identifier

sp8n5.pzcs  
lpf25.imp  
73  
151  
151  
1  
33  
4  
4.0000  
9000  
sp8n5.pz

PUBLICATIONS

- 1) J.I. Aunon, C.D. McGillem and R.D. O'Donnell, "Comparison of Linear and Quadratic Classification of Event Related Potentials on the Basis of Their Exogenous or Endogenous Components," Psychophysiology: 19:531-537
- 2) C.D. McGillem, J.I. Aunon and C.A. Pomalaza, "Improved Waveform Estimation Procedures for Event Related Potentials," accepted for publication, IEEE Transactions of Biomedical Engineering
- 3) C.D. McGillem, D.B. Yu and J.I. Aunon, "Effects of Ongoing EEG on Latency Measurements of Evoked Potentials," IEEE Engineering on Medicine and Biology Conference, Sept. 1982, Philadelphia
- 4) J. Moser, J.I. Aunon and C.D. McGillem, "Classification of Event Related Brain Potentials," Proc. ACEMB Conference, Philadelphia, Sept. 1982
- 5) K.B. Yu and C.D. McGillem, "Optimum Filters for Estimating Evoked Potentials Waveforms," IEEE Transactions of Biomedical Engineering, Nov. 1983

PROFESSIONAL PERSONNEL  
Principal Investigators

Clare D. McGillem, Ph.D. Professor of Electrical Engineering  
Jorge I. Aunon, D.Sc.. Associate Professor of Electrical Engineering

DEGREES AWARDED

Kai-Bor Yu, Ph.D. Thesis: "Optimum Time Varying Filters for Transient Waveform Analysis, May, 1982.